Single-cell RNA sequencing of the holothurian regenerating intestine reveals the pluripotency of the coelomic epithelium

Joshua G. Medina-Feliciano[1], Griselle Valentín-Tirado[1], Kiara Luna-Martínez[1], Yamil Miranda-Negrón[1], José E. García-Arrarás[1*]

[1] Department of Biology, University of Puerto Rico, Río Piedras, San Juan, PR

* Corresponding author

Email: jegarcia@hpcf.upr.edu

Abstract

In holothurians, the regenerative process following evisceration involves the development of a “rudiment” or “anlage” at the injured end of the mesentery. This regenerating anlage plays a pivotal role in the formation of a new intestine. Despite its significance, our understanding of the molecular characteristics inherent to the constituent cells of this structure has remained limited. To address this gap, we employed state-of-the-art scRNA-seq and HCR-FISH analyses to discern the distinct cellular populations associated with the regeneration anlage. Through this approach, we successfully identified thirteen distinct cell clusters. Among these, two clusters exhibit characteristics consistent with putative mesenchymal cells, while another four show features akin to coelomocyte cell populations. The remaining seven cell clusters collectively form a large group encompassing the coelomic epithelium of the regenerating anlage and mesentery. Within this large group of clusters, we recognized previously documented cell populations such as muscle precursors, neuroepithelial cells and actively proliferating cells. Strikingly, our analysis provides data for identifying at least four other cellular populations that we define as the precursor cells of the growing anlage. Consequently, our findings strengthen the hypothesis that the coelomic epithelium of the anlage is a pluripotent tissue that gives rise to diverse cell types of the regenerating intestinal organ. Moreover, our results provide the initial view into the transcriptomic analysis of cell populations responsible for the amazing regenerative capabilities of echinoderms.

Introduction

Animals exhibit a remarkable diversity in their responses to injury, ranging from basic wound healing to the complete regeneration of lost structures. At one end of the spectrum are species that heal wounds without regenerating the missing part, while at the other end are those capable of recreating structures identical to the original. Despite these differences, all animals possess some level of regenerative ability. This capacity for regeneration can vary not only between different species but also within the same species, depending on the tissue or organ involved.

For decades, scientists have tried to understand these vast differences in regeneration capacities across the animal kingdom. For this they have focused on those species that show amazing regenerative abilities (Tanaka and Reddien, 2011), including coelenterates (hydra) (Vogg et al., 2019), flatworms (planaria) (Reddien, 2018), fish (zebrafish) (Gemberling et al., 2013) and amphibians (axolotl) (Roy and Gatien, 2008) among others. These studies have uncovered various mechanisms that regeneration-competent species exhibit to regenerate tissues, entire organs, body parts, and in some cases complete bodies. Key findings include the discovery of essential processes, such as the formation of a blastema – a mass of proliferating cells that plays a crucial role in regenerating the lost structure (Min and Whited, 2023; Poleo et al., 2001; Santos-Ruiz et al., 2002; Seifert and Muneoka, 2018; Stocum, 2004; Zenjari et al., 1996).

Among deuterostomes, echinoderms are considered prime exponents of regenerative capability (Candia-Carnevali et al., 2024). Within this group, holothurians, commonly known as sea cucumbers, exhibit an extraordinary form of regeneration. They can regenerate their internal organs following evisceration, a process in which they expel their viscera in response to stress or predation (Byrne, 2023). This extraordinary ability makes them a valuable model for studying regeneration in complex organisms. The regeneration of the digestive system in holothurians, in particular, has garnered significant interest (Dolmatov, 2021; Mashanov et al., 2014; Medina-Feliciano and García-Arrarás, 2021; Quispe-Parra et al., 2021; Su et al., 2022). Upon evisceration, the holothurian intestine, which constitutes nearly their entire digestive tract, begins to regenerate from the mesentery, a supportive tissue layer where the original intestine was attached (García-Arrarás et al., 1998). A thickening at the injured end of the mesentery, known as an “anlage” or “rudiment,” initiates this process (García-Arrarás et al., 1998). This structure is analogous to a

blastema but differs in that the cell proliferation mainly occurs in the surrounding epithelium, rather than in the mesenchymal cells, as observed in classical blastemas (Carlson, 2007; García-Arrarás et al., 1998).

Histologically, the holothurian intestinal anlage forms from dedifferentiated cells within the mesentery, which revert to a more stem-cell-like state before proliferating and migrating to form a new intestinal structure (Candelaria et al., 2006; Mashanov et al., 2005). This dedifferentiation process is crucial for regeneration, involving a spatial and temporal gradient starting at the injury site and extending along the mesenteric border (García-Arrarás et al., 2011). The new epithelial layer that forms around the anlage is distinct from the original mesothelium, shows significant morphological and molecular changes compared to the mesenteric tissue (Candelaria et al., 2006; García-Arrarás et al., 1998; Mashanov et al., 2005). Further examination of holothurian regeneration reveals that most cellular division occurs within the anlage's coelomic epithelium (García-Arrarás et al., 2011, 1998). These proliferating cells are hypothesized to differentiate into various cell types, including myocytes and neurons, as well as mesenchymal cells, through an epithelial to mesenchymal transition (EMT) (García-Arrarás et al., 2011, 1998). The gene expression profiles during the formation and growth of the anlage suggest extensive reprogramming, leading to a more plastic cell phenotype (Ortiz-Pineda et al., 2009; Quispe-Parra et al., 2021; Rojas-Cartagena et al., 2007).

The process of intestinal regeneration in holothurians raises fundamental questions of regenerative phenomena particularly concerning the identity, origin, and fate of progenitor cells, involved in the process (Alvarado and Tsonis, 2006; Candia-Carnevali et al., 2024). In this context, the role of the anlage, and specially the mesothelium (also named celothelium) in echinoderms, deserved particular attention (Candia-Carnevali et al., 2024; Smiley, 1994). This tissue, mainly composed of coelomic epithelia and myocytes, exhibit significant morphological and gene expression changes that are associated with the dedifferentiation process. These dedifferentiated cells form the coelomic epithelium of the anlage and appear to be the principal source of cells for the new intestine. Despite these findings, little is known about the cell composition and dynamics of the anlage nor of its coelomic epithelium.

92 Single-cell omic studies offer tremendous promise to dissect the cellular contributions of the holothurian intestinal
93 anlage and to identify the specific cells involved in generating a new intestine. Single-cell RNA sequencing (scRNA-
94 seq) a powerful tool for dissecting cellular composition and dynamics has been used in related species to explore
95 regenerating or developing tissues. In mice, for instance, scRNA-seq has been employed to investigate the
96 response to injury. However, these studies have primarily focused on tissue healing rather than the full regenerative
97 process (Ayyaz et al., 2019; Beumer and Clevers, 2021; Capdevila et al., 2021; Parigi et al., 2022). Beyond healing,
98 scRNA-seq has been pivotal in studying regenerating systems such as the axolotl limb blastema and planarian
99 regeneration providing a detailed insights into the cellular processes at play (Gerber et al., 2018; King et al., 2024;
100 Leigh et al., 2018; Rodgers et al., 2020). Furthermore, considering the close relationship between regeneration and
101 embryogenesis, scRNA-seq, has also been used to understand the cellular events in developing echinoderm
102 embryos (Cocurullo et al., 2023; Paganos et al., 2022a, 2022b, 2021; Satoh et al., 2022; Tominaga et al., 2023).
103 These applications highlight the groundbreaking role of scRNA-seq in advancing our knowledge of the cellular
104 mechanisms in both regenerative and developmental contexts.

105

106 In this study, we employ scRNA-seq to analyze the regenerating intestinal anlage of the sea cucumber *Holothuria*
107 *glaberrima*, aiming to delineate its constituent cellular populations (Fig 1A). We corroborate our findings using
108 hybridization chain reaction fluorescent in situ hybridization (HCR-FISH) to verify the presence and location of
109 specific cell types (Choi et al., 2018). The results provides transcriptomic evidence on the pluripotency of the anlage
110 coelomic epithelia and the first description of the holothurian regenerating precursor cells. This research not only
111 advances our understanding of the unique regenerative capabilities of holothurians but also contributes to the
112 broader field of regenerative biology, highlighting the diverse strategies employed by different organisms to restore
113 lost tissues.

114

Results

Previous work from our laboratory has shown that the rudiment or anlage that forms at the tip of the mesentery plays a pivotal role in the formation of the new intestine (García-Arrarás et al., 2019). This transient mass of cells is thought to give rise to most intestinal cell types, the sole exception being the luminal cells. Therefore, to maximize the characterization of the cells in the regenerative anlage, we chose to perform scRNA-seq in the tissues of 9-days post evisceration (dpe) regenerating animals (García-Arrarás et al., 2011, 1998). At this stage a well-formed anlage consists of epithelial cells surrounding a large area of connective tissue populated with mesenchymal cells (Fig 1A). More importantly, different cell populations undergoing proliferation or differentiation can be found at this stage. Since some of the cellular processes during regeneration occur in a spatio-temporal gradient along the length of the mesentery, we separately surveyed the anlage and the mesentery tissues accordingly. Thus, for each animal, the anlage was separated from the mesentery, and both tissues were processed independently, for a total of four scRNA-seq runs.

Tissues were treated with 0.05% trypsin for 15 min and cells were dissociated manually. The dissociated cells were counted and used for the scRNA-seq analyses. Additionally, samples from the cell dissociation were fixed in poly-lysine treated slides and analyzed with immuno- and cyto-chemical techniques. Therefore, these cells correspond to the same batch whose transcriptomes were sequenced.

Cell Heterogeneity: Immuno- and cyto-chemical analyses

The strength of the scRNA-seq data depends mainly on the dissociation and isolation of the cell populations from the dissected tissue. Since our focus was on the cells of the regenerating anlage, we devised a dissociation protocol that favored the isolation of the cells within this structure. To determine, at least partially, the cell types in our original dissociation, we performed immuno- and cyto-chemical analyses on the enzyme-dissociated cell suspension that was used for the scRNA-seq. The labeling obtained for each marker is shown in S1 Fig.

142 We found that, in the dissociated anlage, 5% of the cells were labeled with a spherulocyte (immune cell) marker, 2-
143 7% with phalloidin (a muscle marker), 40% with a mesenchymal marker (KL14-antibody), and a large number of
144 cells (32-60%) with a mesothelial marker (MESO-antibody). Similar populations were found in the mesentery,
145 although in this tissue, 5-10% of cells expressed the neuronal markers, heptapeptide GFSKLYFamide (Diaz-
146 Miranda et al., 1995) and RN1 (Diaz-Balzac et al., 2007). This analysis suggested that most of the cells originate
147 from the regenerate coelomic epithlium.
148
149 Different populations were also observed with three different tubulin antibodies (S2 Fig). In the 9-dpe anlage, anti-
150 acetylated alpha tubulin labeled about 7% of the cells, anti-beta tubulin labeled about 70% of the cells, while an anti-
151 alpha tubulin labeled about 80% of the cells. Except for the acetylated alpha tubulin, which labeled about 1% of the
152 cells dissociated from the mesentery versus 7% of those from the anlage, anti-alpha and beta labeling percentages
153 were similar in both mesentery and anlage dissociated cells.
154
155 Finally, a cell population labeled with fluorescently-labeled phalloidin accounted for about 7% of the cells in both
156 mesentery and anlage. These cells, however, did not correspond to the elongated muscle cells of the mesentery.
157 Instead, they were rounded cells with labeling found in the cytoplasm surrounding one side of the nuclei.
158
159 Two cell populations from the mesentery are not represented or are greatly underrepresented in the scRNA-seq.
160 Firstly, the muscle cells of the mesentery, due to their non-dissociation by the protocol used, were absent in the
161 dissociated cell suspension. Their elongated morphology would have further complicated their passage via cell
162 separation system for sequencing. Secondly, the majority of neurons from the neuronal network associated with the
163 mesentery could not be dissociated (Nieves-Ríos et al., 2020). We did, however, observe structures that resembled
164 a tangled mass of cells immunoreactive to some of our neuronal markers. This suggests that the mesentery nervous
165 component, being unable to be isolated as single cells, was not sequenced.
166
167 In summary, the immuno- and cytochemical results show that the dissociated cell populations sequenced
168 correspond to cellular phenotypes that have been previously described within the regenerating anlage. The
169 abundance of these cells in the sequenced samples corresponds to the ease of their dissociation by trypsin. Thus,

dedifferentiated cells of the mesentery and anlage epithelium (which are loosely connected to each other) and those of the connective tissue are probably over-represented compared to differentiated cell types.

Cell populations defined by scRNA-seq

Analysis of scRNA-seq data resulted in a total of 3,844 cells, with 2,392 originating from the two anlage samples and 1,452 from the two mesentery samples. Upon dataset integration and graph-based clustering, we identified 13 clusters, each thought to represent singular cell types or cell states in the regenerating intestine (Fig 1A-B). The percentage of cells that form each cluster differs from cluster to cluster, ranging from 21% (cluster 0) to 1% (cluster 12) of the total cells. Nonetheless, each cluster consists of cells from both the mesentery and anlage samples (Fig.

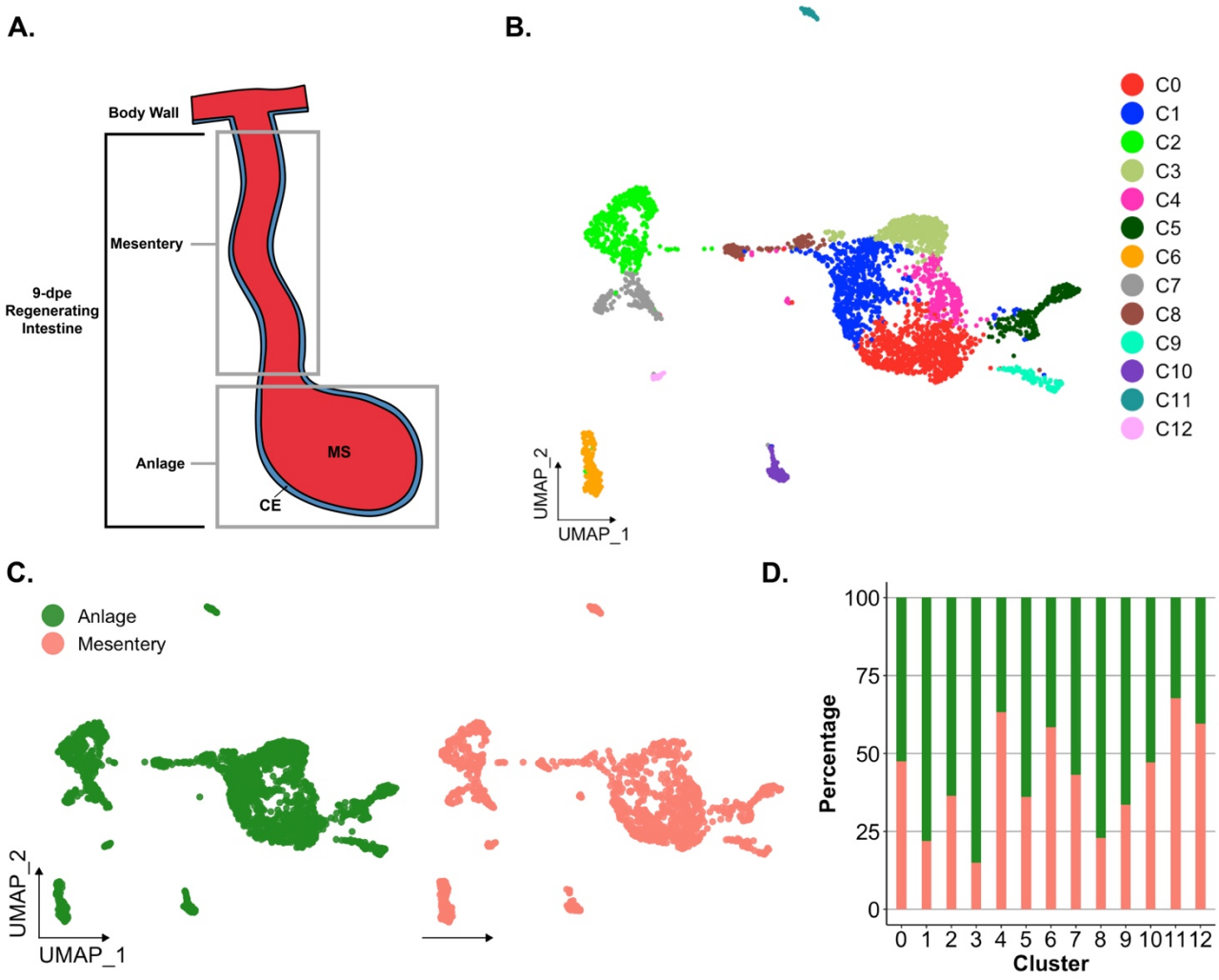

Fig 1. Overview of single cell RNA sequencing of regenerating intestinal tissue of *H. glaberrima*. (A) Diagram of 9-day regenerating intestine depicting mesentery and anlage components (B) UMAP plot of population identities determined through unsupervised clustering of 9-day regenerating mesentery and anlage tissues. (C) Representation of cells per tissue of both samples. (C) UMAP projections of cluster cells separated by tissue of origin. (D) Percentage of cells per cluster based on their tissue of origin.

180 1C & D). The number of clusters did not change dramatically under various parameters (resolution, dimensionality,
181 and number of variable features), constantly around 12-15 clusters. Moreover, except for C3 and C4, the clusters
182 are supported by the clustering significance analysis performed with scSHC (Grabski et al., 2023), a model-based
183 hypothesis testing method for scRNA-seq that evaluates the probability of each individual cluster being unique (S3
184 Fig). The uniqueness of C3 and C4 is suggested by additional analyses as will be addressed below.
185
186 Each identified cluster exhibits a distinctive gene expression profile relative to cells in other clusters (Fig 2). The top
187 expressed gene serves as a marker for each cell population to highlight the uniqueness of each cluster. In Fig 2, we
188 show the relative expression of the top gene for each cluster based on two factors: (1) difference in percentage of
189 representation and (2) $\log_2$ fold-change ($\log_2$FC) against all other clusters. Interestingly, each cluster shows
190 dramatic differential expression values (> 2 $\log_2$FC) and differences in representation percentages over 50%, except
191 for C0 through C3, with differences in representation around 30%.
192
193 Prior to characterizing each of the 13 cell clusters, we sought to understand what, in a broad view, appears to be a
194 segregation of ~90% of the cells into two distinct supra-clusters. One of them encompassing 7 clusters (C0, C1, C3,
195 C4, C5, C8, C9) that corresponded to 69.6% of all cells and the other encompassing two clusters (C2 and C7) that
196 corresponded to 19.1% of cells. The remaining 11.3% of cells were distributed in 4 distinct isolated clusters (C6,
197 C10, C11, and C12). As stated earlier, all clusters have representation from mesentery and anlage tissues (Fig 1C-
198 D), thus excluding the possibility that the two supra-clusters represented mesentery versus anlage cells.

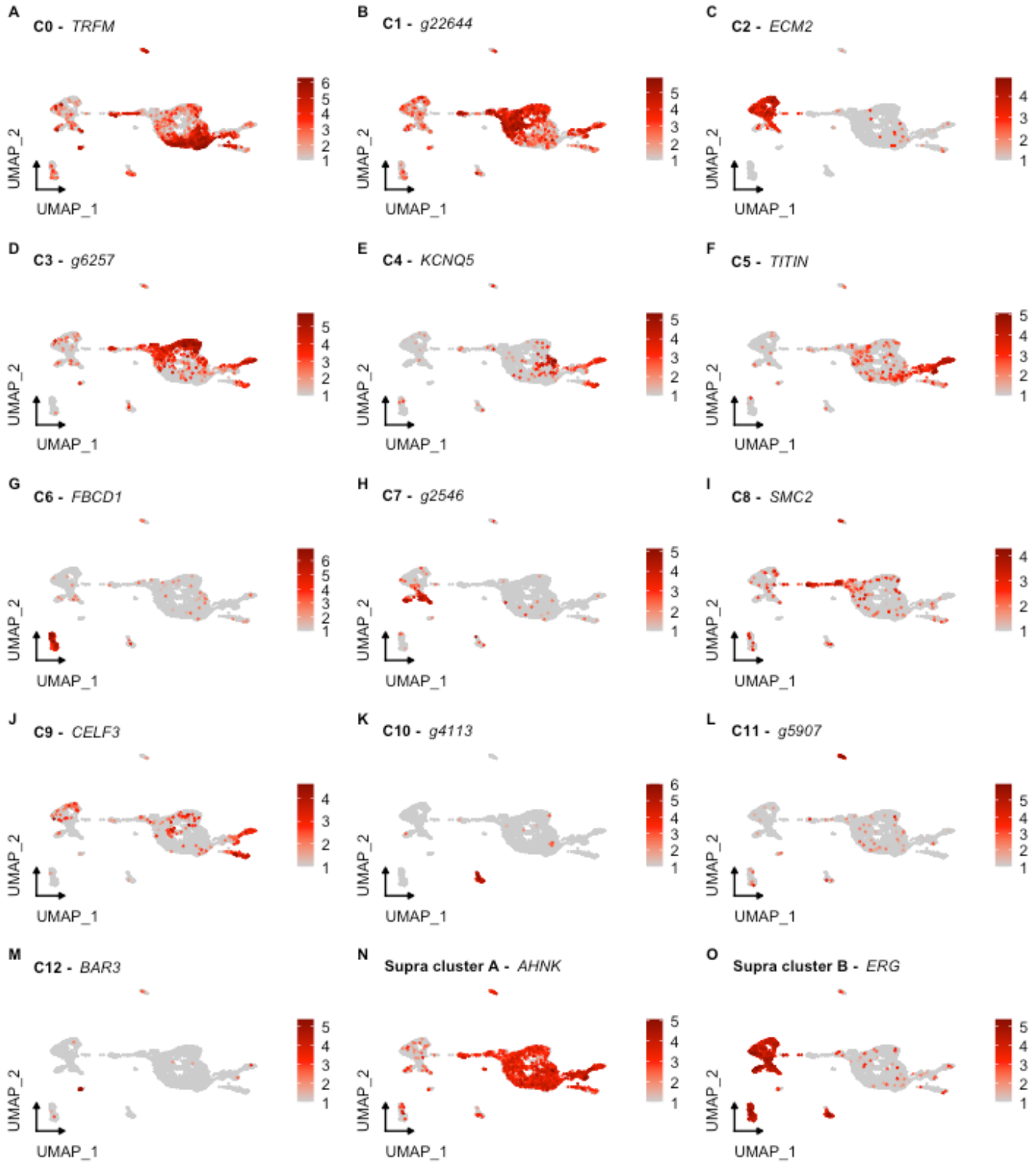

Fig 2. UMAP visualization of clusters highlighting the expression of their top genes. Each gene corresponds to the top gene of each independent cluster based on the percentage of representation to other clusters.

Mesenchymal versus Epithelial Clusters

These two supra-clusters are of interest as they appear to represent the two main cell types found in the regenerating intestine: coelomic epithelial cells and mesenchymal cells (Fig 1B). Understanding the cell types that correspond to each cluster is essential as cellular processes crucial for regeneration are thought to be localized to the coelomic epithelia of the regenerating anlage. Comparison between these two supra-clusters showed distinct expression profiles that allowed us to characterize their cell types. For instance, the supra-cluster composed of C2 and C7, showed *ERG* (transcriptional regulator ETS-related gene) as the top expressed gene, an oncogene that is related to embryonic development, differentiation, angiogenesis, and apoptosis (Dhordain et al., 1995; Iwamoto et al., 2001; Vlaeminck-Guillem et al., 2000) (Fig 2). More importantly, the expression of *ERG* has been associated with mesenchymal identity in other echinoderms (Meyer et al., 2023; Tominaga et al., 2023). In these studies, *ERG* has been reported as the marker gene of mesenchymal cells of sea urchin and sea star larva by scRNA-seq analyses and the localization of *ERG* on embryonic precursor mesenchymal cells of the sea urchin was further confirmed by *in situ* analyses (Meyer et al., 2023). In addition, this latter group also reported these mesenchymal cells to express a GATA transcription factor (*GATA3*) and *ETS1*, which in our dataset are also being expressed only by populations within this supra-cluster (*GATA2* and *ETS1* – Fig 3B). The gene *ETS1* has been associated with the differentiating sea urchin larvae mesenchymal cells and has a vital role in EMT and cellular invasion of mesenchymal cancer cells (Gluck et al., 2019; Koga et al., 2010; Meyer et al., 2023). The expression of *PRG4* (proteoglycan-4) reinforces the mesenchymal identity of this supra-cluster in the regenerating intestine (S4 Fig), which correlates with previous studies that have identified a proteoglycan-like molecule in the mesenchyme of 7-dpe regenerating intestine (Vázquez-Vélez et al., 2016).

In contrast, the top marker gene in the other supra-cluster is *AHNK*, known as neuroblast differentiation-associated protein AHNAK. Reports have shown *AHNK* to have a role in calcium regulation, cellular migration, and carcinogenic transformation of colon epithelial cells (Dumitru et al., 2013). Furthermore, this gene is overexpressed in regenerating rat muscle compared to normal muscle (Huang et al., 2007). However, the localized expression of *WNT9* in the C1, C3, C5, and C8 of this supra-cluster more clearly favors its classification as a marker for coelomic epithelial cell types (Fig 3B and S4 Fig). A previous study from our laboratory using *in situ* hybridization, details the expression of *WNT9* during intestinal regeneration in *H. glaberrima,* where it was shown to be localized to the

229 coelomic epithelium of the anlage and adjacent mesentery (Mashanov et al., 2012). In addition, correlating with what
230 was shown by the *in situ* hybridization results, the population of cells that differentially expresses *WNT9* makes 15%
231 of those in the mesentery. However, it is close to 30% of the cells in the anlage. Additional analyses, discussed
232 below, further strengthens the coelomic epithelium identity of cells in this supra-cluster.

233

234 In summary, results show 13 individual cell clusters with distinct expression profiles in the regenerative intestinal
235 tissue. Moreover, our results suggest a principal separation of clusters based on whether they correspond to those
236 of the mesenchyme or to cells from the coelomic epithelia layer. The rest of the populations show top expressed
237 genes that are immune-related suggesting that these must be coelomocyte populations (Fig 2).

238

239 *Cluster Identities*

240
241 Rather than considering single genes, the uniqueness of each cluster can be assessed in terms of their
242 transcriptomic profile (Fig 3A) and by the expression of transcription factors and intercellular signaling molecules
243 (Fig 3B). As shown in Fig 3A-B, each cluster has a unique transcriptomic profile. Nonetheless, some clusters show
244 their close relationship (epithelial vs mesenchymal) based on shared gene expression or representation. A notable
245 example is clusters C0, C1, C3, and C4 of the epithelial layer populations, which share many top genes, albeit at
246 different expression levels. Similarly, C8 and C9 have low expression of genes expressed by C0, C1, C3 and C4 but
247 have expression of other genes that are not expressed by any other cluster. This is also true for the mesenchymal
248 clusters, where these two clusters have overlap of some genes, that are not expressed by other clusters. Therefore,
249 these results show the interaction of these clusters and their transcriptomic relationship depending on where they
250 are localized within the regenerating intestinal tissue.

251

252 Identifying the top genes expressed by each cluster also provides essential, notwithstanding limited, information for
253 their complete identification. To further characterize each cluster, we have used other analyses or performed
254 additional experiments, including (1) multiple gene expression patterns, (2) enriched ontology, (3) HCR-FISH and
255 (4) pseudo-trajectory. Initially, we describe in depth the potential identity of these clusters based on their expression
256 pattern and enriched ontology, and we will end with their potential interactions.

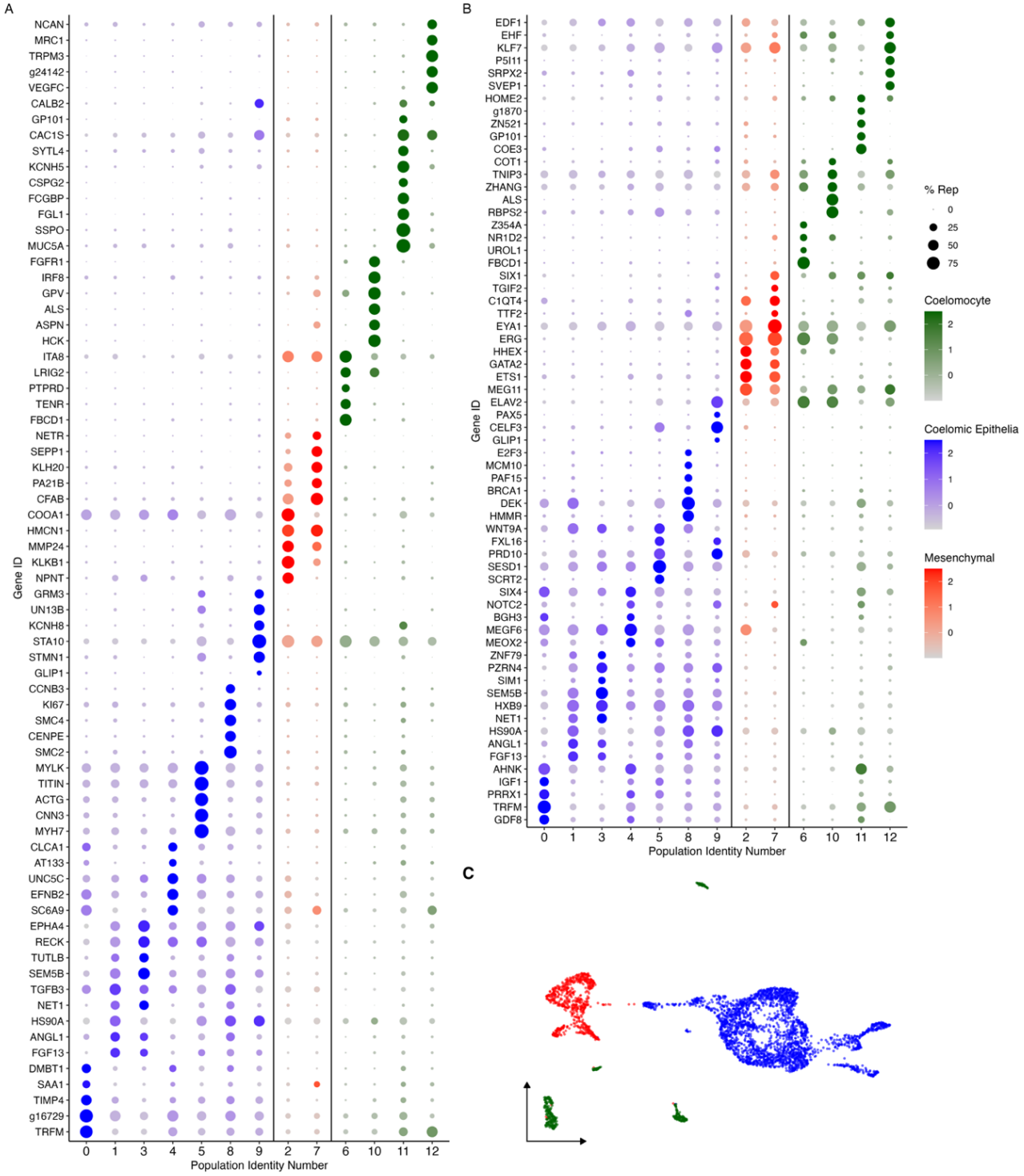

Fig 3. Cluster characterization by gene expression. (A) Top-expressed genes or (B) genes corresponding to transcription factors and intercellular signaling molecules are identified in the 13 cell clusters. Clusters are classified by their corresponding cell type, where blue corresponds to cells of the coelomic epithelium, red to those in the mesenchyme and green to coelomocytes. Color intensity shows the expression level of each gene in $\log_2$fold-change ($\log_2$FC) values. Dot size corresponds to percentage of representation of the gene in the respective cluster compared to all others. Gene identifiers starting with "g" correspond to uncharacterized gene models of *H. glaberrima*. (C) UMAP plot of clusters colored by cell type.

An in-depth analysis of the various clusters and their possible relation to cell populations

Coelomocyte populations

Coelomocytes are specialized cells found in the coelomic fluid and within organs of echinoderms. These cells have been associated with immunological roles including pathogen recognition, encapsulation, phagocytosis, debris removal, cytokine production and secretion among others (Barela Hudgell et al., 2022; Courtney Smith et al., 2018; García-Arrarás et al., 2006; Smith et al., 1995), In holothurians, these cells have been shown to be present at injury sites and in the regeneration anlage. Coelomocytes can be subdivided into different populations by using morphological, physiological, and molecular characteristics (Ramírez-Gómez et al., 2010).

Many of the coelomocyte characteristics correlate with the top differentially expressed genes of cell populations within our data. These immune-like clusters (C6, C10, C11, and C12) have high expression of genes related to the immune system that are not shared with any other cluster. For example, C6 embodies a distinct cell population that represents a substantial number of cells (6% of all cells, 8% of the mesentery and 4% of the cells in the anlage). These cells are the only population expressing *FBCD1* (fibrinogen C domain-containing protein 1). Cells in C6 also express other genes such as various tyrosine protein phosphate receptors, integrin alpha-8 (*ITA8*), platelet glycoprotein V (*GPV*), leucine rich repeats and immunoglobulin-like domains protein 2 (*LRIG2*) (Fig 4A). The immune identity of C6 is also supported by the resulting gene set enrichment of gene ontology (gseGO) terms related to immune responses, such as *ubiquitin-dependent ERAD pathway*, *innate immune response activating cell surface receptor signaling pathway*, *respond to endoplasmic reticulum stress*, *phagocytosis* and many more related to defense mechanisms (Fig 4B). Similarly, C10 and C12 transcriptomic profiles suggest they correspond to immune-like populations (Fig 4C). Specifically, C10 shows various uncharacterized genes along with *HCK* (tyrosine-protein kinase HCK), *DMBT1* (deleted in malignant brain tumors 1), *ALS* (insulin-like growth factor binding protein complex acid labile subunit), *GPV*, and *IRF8* (interferon regulatory factor 8), *FER* (tyrosine-protein kinase Fer). The top GO enriched terms of this cluster support its involvement in immune process, some of these being: *lipase activity regulation*, *Fc receptor mediated stimulatory signaling pathway*, *cellular pigmentation*, *B cell activation involved in immune response*, and *Fc receptor signaling pathway*. The transcripts expressed by C12 show a more complex profile, where most of the top genes are uncharacterized. Nonetheless, among the annotated genes are

288 *BAR3* (Balbiani ring protein 3), *LYS1* (lysozyme 1), *TRPM3* (transient receptor cation channel subfamily M member
289 3), *PGCA* (aggrecan core protein) and *MRC1* (macrophage mannose receptor 1). The top genes of C11 include a
290 great number of immune genes such as *MUC5A* (mucin-5AC), *FCGBP* (IgGFc-binding protein), *SSPO* (SCO-
291 spondin), *FCN1A* (ficolin-1-A), *MUC5B* (mucin-5B), and *TIE1* (tyrosine-protein kinase receptor Tie-1). However, the
292 top genes of this cluster also include several genes involved in neuronal activity, which is evident in the top enriched
293 GO terms of this cluster that include *regulation of postsynaptic membrane potential*, *excitatory postsynaptic*
294 *potential*, *chemical synaptic transmission*, *endoplasmic reticulum to Golgi vesicle-mediated transport*, *adult*
295 *behavior*, and *regulation of neurotransmitter levels* (Fig 4A-B).
296
297 To partially confirm the prediction that cells from C6, C10, C11 and C12 corresponded to coelomocyte populations,
298 we used HCR-FISH to identify the cell types expressing the top gene in one of the clusters. We focused on the
299 expression of *FBCD1*, the gene that is the most represented by cells of C6. *In situ* hybridization identified a distinct
300 cell type in both regenerating and non-regenerating tissues (Fig 4D-E). These cells showed round or oval
301 morphologies with a central round nucleus. In some cases, short extensions could be observed. The cells were
302 heterogeneously distributed in all tissues, including the nervous system and the body wall, and could be found
303 associated with either epithelial tissues or with the extracellular matrix (ECM) in the normal intestine, the intestinal
304 anlage and in the mesentery of normal or regenerating animals. The widespread distribution of this cell type hinted
305 at a cell function consistent with patrolling the body to detect and respond to potential threats such as injury or
306 bacterial invasion.
307
308

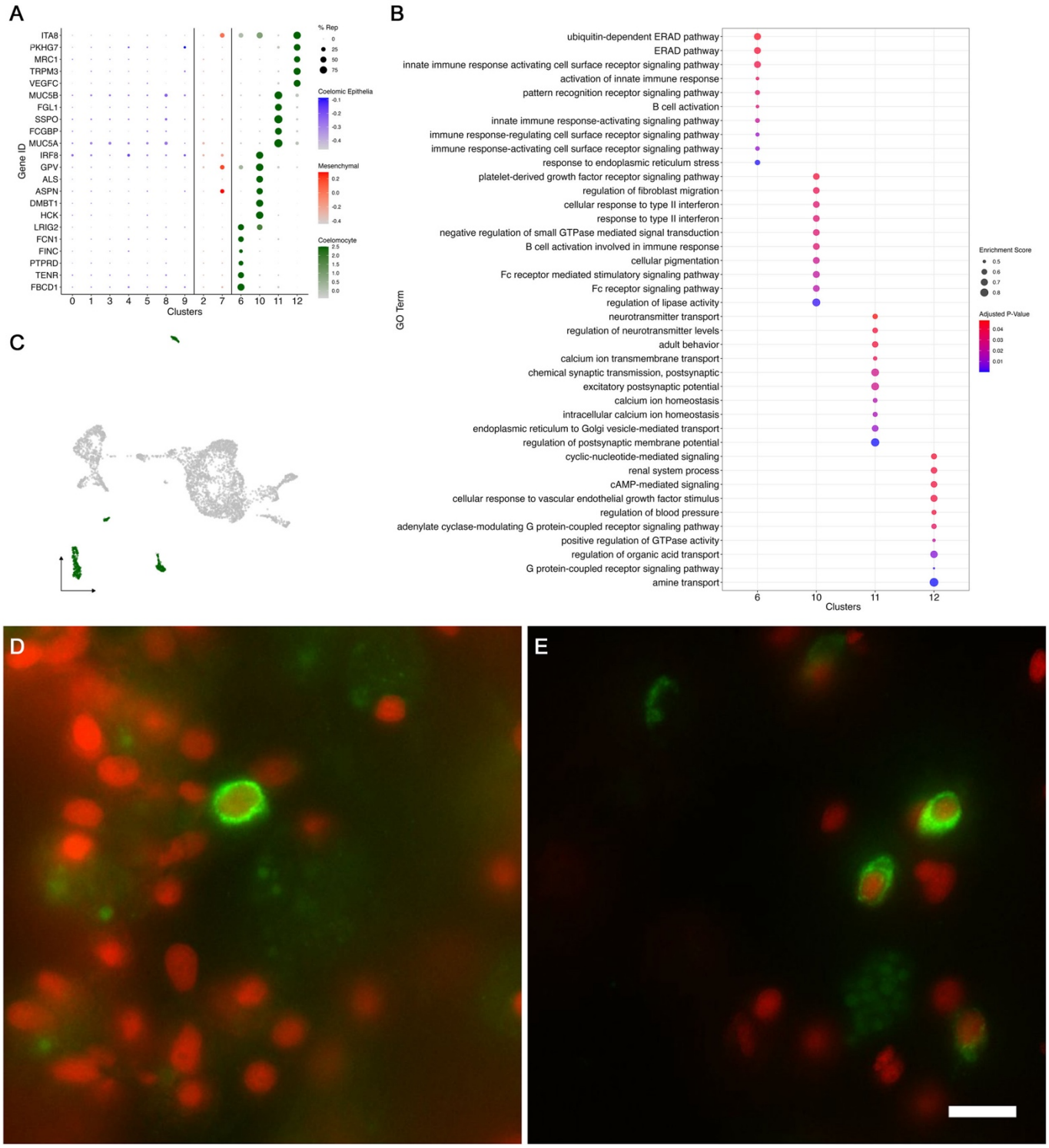

Fig 4. Expression profile of coelomocyte cell types. (A) Dot plot showing the top expressed genes of C6, C10, C11, and C12. Color intensity reflects the expression levels in $\log_2$FC values. Dot size correspond to the percentage of representation of each gene in the respective cluster compared to all others. (B) Top enriched GO biological processes terms of C6, C10, C11, and C12. Dot size corresponds to the enrichment score while the color reflects the adjusted p-value. (C) UMAP highlighting the coelomocyte populations. (D-E) HCR-FISH for *FBCD1* in holothurian intestinal tissues. Cells expressing *FBCD1* mRNA in the connective tissue layer of (D) regenerating mesentery and (E) normal intestine of *H. glaberrima* are shown. Red = DAPI stain, green = HCR-FISH. Bar= 10 µm.

311 ### *Mesenchymal cell populations*

312

313 Mesenchymal cells of the intestinal anlage are yet to be well studied. They are known to be less proliferative than
314 those in the overlying epithelium (García-Arrarás et al., 2011, 1998) and involved in ECM remodeling (Quiñones et
315 al., 2002). Some of the mesenchymal cells are thought to migrate from the connective tissue of the mesentery
316 (Cabrera-Serrano and García-Arrarás, 2004), while others have been shown to originate via EMT from the overlying
317 epithelium (García-Arrarás et al., 2011). Some of these cells will form a mesenchymal cellular layer associated with
318 the luminal epithelial cells as the lumen forms (García-Arrarás et al., 2011). As explained earlier, we have proposed
319 that C2 and C7, form a separate supra-cluster, clearly identified by the increased expression of *ERG* with 5 of
320 $\log_2$FC and a 90% representation (Fig 2O). These two clusters also share many marker genes, including multiple
321 ECM genes (Fig 5D). For instance, highest expressed gene of C2 is *TIMP3* (metalloproteinase inhibitor 3), followed
322 by *NPNT* (nephronectin), which has been reported to be an integrin ligand during kidney development (Sun et al.,
323 2018). Additionally, this cluster has overexpression of *ECM2* (extracellular matrix protein 2), *KLKB1* (plasma
324 kallikrein), *MMP14* (matrix metalloproteinase 14), *MMP24* (matrix metalloproteinase 24), *HMCN1* (hemicentin-1),
325 and *ITA8* (integrin alpha-8), all of which are explicitly related to extracellular matrix component (Bokel and Brown,
326 2002; Dolmatov and Nizhnichenko, 2023; Dong et al., 2006; Stamenkovic, 2003; Volkert et al., 2014). Many of these
327 genes are also highly represented in C7. However, here we also find *ITIH2* (inter-alpha-trypsin inhibitor heavy chain
328 H2), *DUOX1* (dual oxidase 1), *SVEP1* (sushi, von Willebrand factor type A, EGF and pentraxin domain-containing
329 protein 1), *SEPP1* (selenoprotein P), and *KLH20* (Kelch-like protein 20) suggesting that cells have gained some
330 specialization and are more advanced in their differentiation when compared to those of C2. Along with this, when
331 analyzing the gseGO, for C2 we obtain GO terms of numerous ECM processes, such as *cell adhesion mediated by*
332 *integrin*, *integrin-mediated signaling pathway*, and *regulation of cell-substrate junction assembly* (Fig 5F). Similarly,
333 C7 has an enrichment of *regulation of cell-matrix adhesion*, *regulation of cell-substrate junction organization*, and
334 *substrate adhesion-dependent cell spreading*. Notably, these clusters also show enrichment of processes involved
335 in cell proliferation, growth, and wound healing. To mention a few for C2 we find *B cell differentiation*, *vascular*
336 *endothelial growth factor receptor signaling*, *regulation of myeloid leukocyte differentiation,* and *negative regulation*
337 *of myeloid cell differentiation*, while C7 shows an enrichment of *positive regulation of wound healing*, *regulation of*
338 *neural precursor cell proliferation*, *positive regulation of response to wounding*, *humoral immune response*,

neuroblast proliferation, among others. This is not surprising considering that this tissue is undergoing active regeneration which requires growth and healing events to be active at distinct stages of the process.

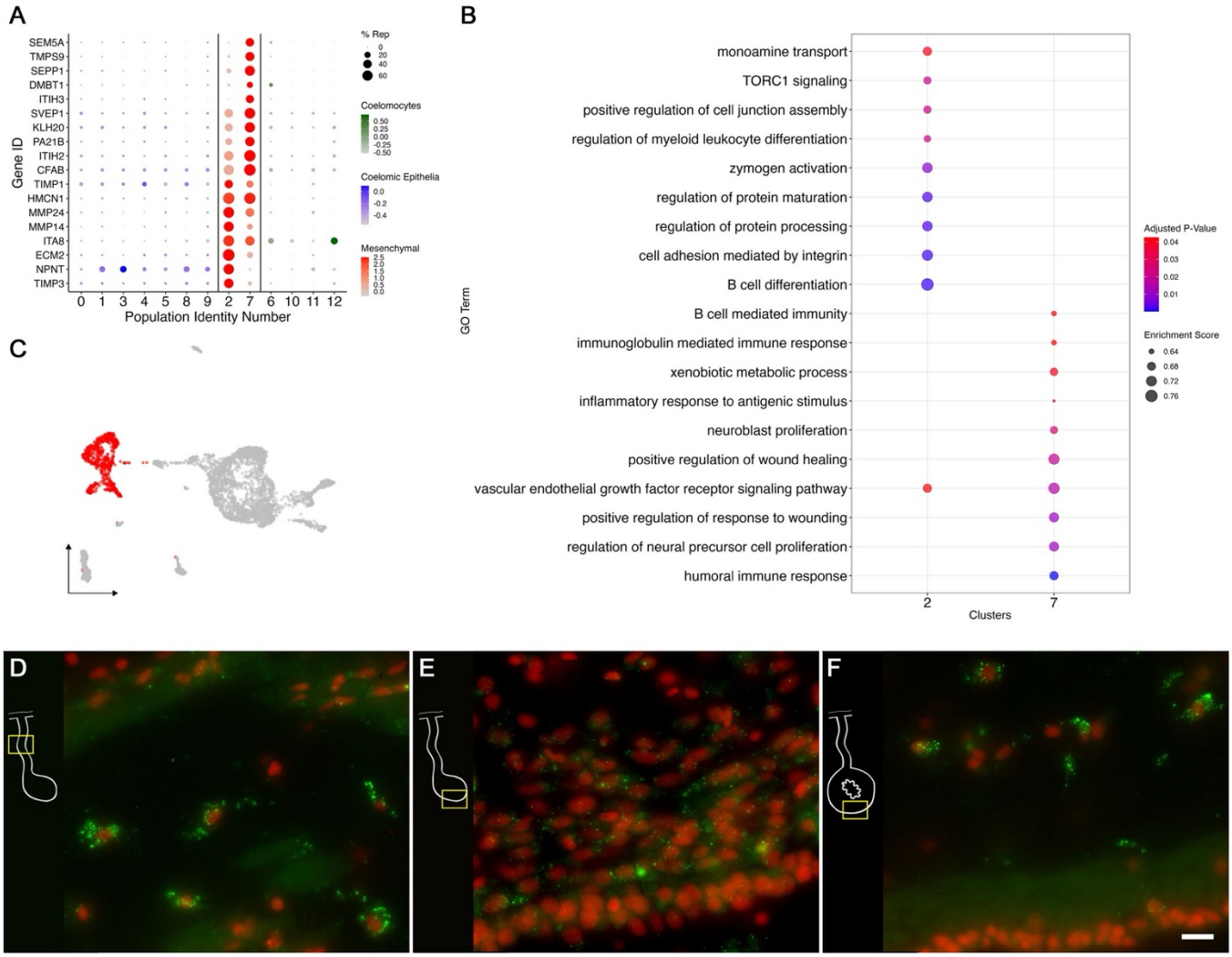

Fig 5. Expression profile of mesenchymal cell types. (A) Dot plot showing the top expressed genes of C2 and C7. Color intensity reflects expression levels in $\log_2$FC values. Dot size correspond to the percentage of representation of each gene in the respective cluster compared to all others. (B) Top GO enriched terms of biological processes of C2 and C7. Dot size corresponds to the enrichment score while the color reflects the adjusted p-value. (C) UMAP highlighting the clusters that correspond to the mesenchymal population (D-F) Cells expressing *HMCNT1* mRNA in the connective tissue layer of (D) regenerating mesentery, (E) intestinal anlage and (F) normal intestine of *H. glaberrima*. Red = DAPI stain, green = HCR-FISH. Bar= 10µm

To confirm our prediction that cells in C2 and C7 were those present within the mesenchyme, we chose to localize the expression of *HMCNT1* mRNA. The mRNA for this protein, known to code for an extracellular protein (Dolmatov and Nizhnichenko, 2023; Lindsay-Mosher et al., 2020; Welcker et al., 2021), is present in both cell clusters. HCR-FISH showed that cells expressing the *HMCNT1* mRNA were present in the connective tissue of the regenerating mesentery and certain regions of the connective tissue of the anlage. In the normal intestine, labeled cells were

347 present in the connective tissue (Fig 5A-C). Cells in the mesentery and normal intestine connective tissue were
348 somewhat distanced from each other and had an irregular morphology with intense labeling throughout the
349 cytoplasm. A weaker labeling was observed in cells of the anlage, which were more densely packed and adjacent to
350 the coelomic epithelium, suggesting that they correspond to cells undergoing EMT on their way to differentiate into
351 ECM-producing mesenchymal cells. A very similar pattern of expression was observed with HCR-FISH for *ERG* (not
352 shown). The ERG-expressing cells were also found in the connective tissue of normal intestine and in the cells of
353 the anlage undergoing EMT.

354 ### *Coelomic epithelia/mesothelial cell populations*

355
356 The mesothelial layer of the intestine and mesentery is formed by cells in contact with the coelomic fluid (coelomic
357 epithelium or peritoneocytes) together with myocytes and neurons. In the regenerating tissues, some of these cells
358 dedifferentiate and form a coelomic epithelia that differs in morphology (Mashanov et al., 2005) and gene
359 expression (Mashanov et al., 2017, 2015, 2012, 2010) to the mesothelium that normally surrounds the organ. This
360 dedifferentiated coelomic epithelium which is present mainly in the anlage and in areas of the adjacent mesentery, is
361 also responsible for most of the cell division that takes place in the regenerating intestine (García-Arrarás et al.,
362 2011). Many of the changes observed in the mesothelium during regeneration take place in a gradient, beginning at
363 the tip of the mesentery (where the anlage forms) and continuing in the adjacent regions of the mesentery
364 mesothelium. Thus, the analysis of the scRNA-seq data in view of our knowledge of the ongoing events in the 9-dpe
365 regenerating organ leads to the conclusion, as stated previously, that the 7 clusters within the major supra-cluster,
366 represent the cells in the coelomic epithelium of the mesentery and the anlage. Here is our analysis:

367

368 **C8 represents the proliferating cells**. These cells mainly found within the anlage coelomic epithelia express
369 proliferation markers such as *PLK1* (serine/threonine-protein kinase PLK1), *SMC2* (structural maintenance of
370 chromosomes protein 2), *PRI2* (PRIM2 - DNA primase large subunit), *PCNA* (proliferating cell nuclear antigen), and
371 *CDK1* (cyclin-dependent kinase 1) (Locard-Paulet et al., 2022). In addition, this cluster has high expression of
372 *TOP2A* (DNA topoisomerase 2-beta), a gene that has also been seen to be overexpressed in proliferating basal
373 cells of the human gastrointestinal epithelia (Busslinger et al., 2021). Other marker genes related to cell mitotic
374 activity found here include *CENPE* (centromere-associated protein E), *SMC4* (structural maintenance of

375 chromosomes protein 4), *K167* (proliferation marker protein Ki-67), and *CCNB3* (G2/mitotic-specific cyclin-B3) (Fig
376 6A). Furthermore, this cluster expresses specific transcription factors such as *E2F3*, *MCM10* (protein MCM10
377 homolog), *PAF15* (PCNA-associated factor) and *BRCA1* (breast cancer type 1 susceptibility protein) that are also
378 associated with control of cell division (Humbert et al., 2000; Lõoke et al., 2017; Xie et al., 2014). The gseGO terms
379 also confirm its proliferative identity with GO terms related to *chromosome separation*, *condensation*, *mitotic*
380 *cytokinesis*, and *regulation of cell cycle checkpoint* (Fig 6B). Moreover, the dividing cell population is higher in the
381 anlage samples (4%) than in the mesentery samples (2%), which is in accordance with what we have observed in
382 regenerating animals, that while cell division does take place in the mesentery, more cells are proliferating in the
383 epithelial layer of the intestinal anlage (Bello et al., 2020; García-Arrarás et al., 2011, 1998).

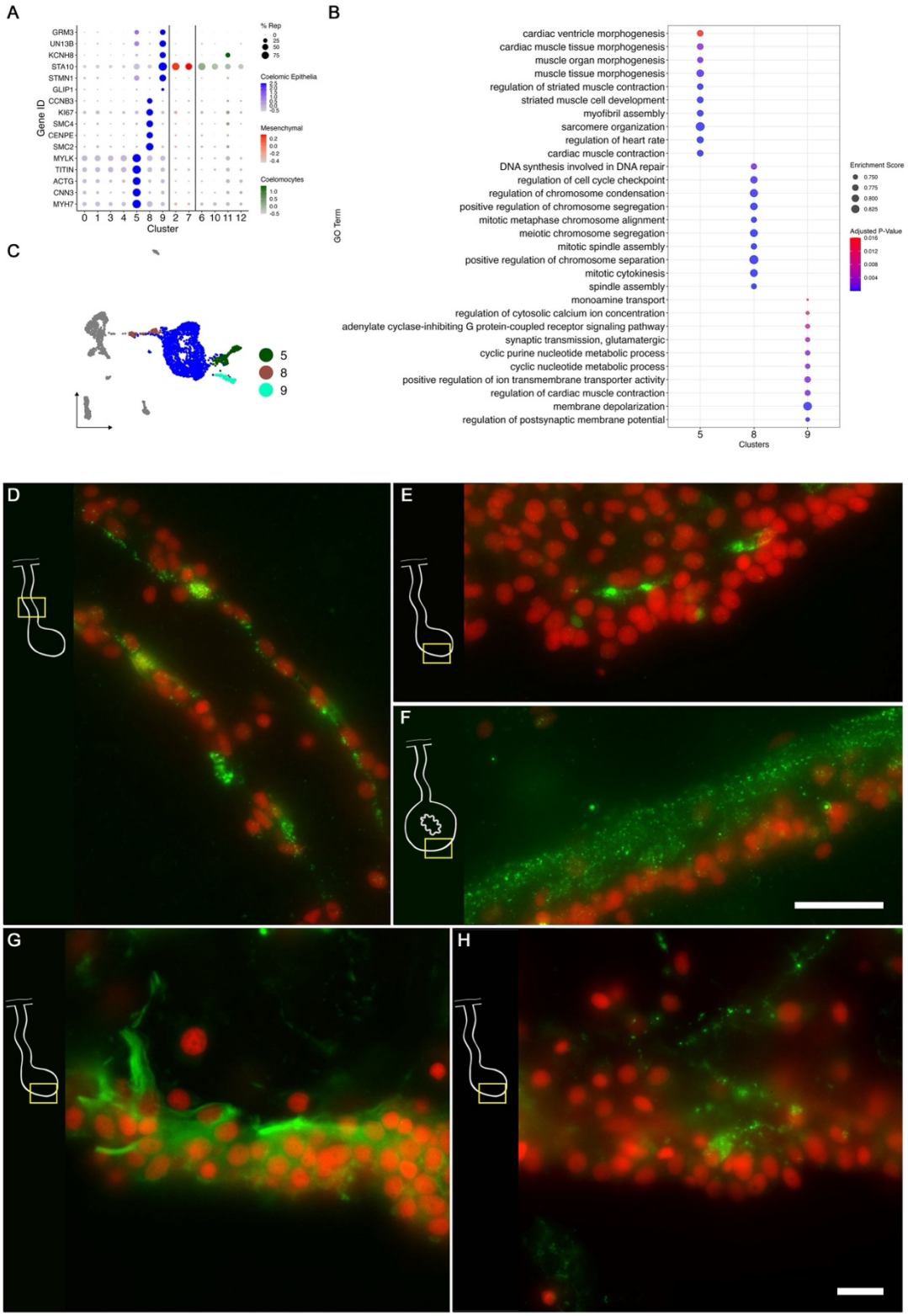

Fig 6. Expression profile of cell clusters undergoing differentiation or proliferation in the coelomic epithelium. (A) Dot plot showing the expression profile of C5, C8, and C9. Color intensity reflects expression levels in $\log_2$FC values. Dot size represents percentage of representation of each gene. (B) Top GO enriched terms of biological processes of each cluster. (C) UMAP highlighting C5, C8, and C9, which along with clusters in color blue correspond to the coelomic epithelium. (D-F) Cells expressing *MYH7* mRNA in the (D) regenerating mesentery, (E) basal area of the anlage coelomic epithelium and (F) muscle layer of the normal intestine. (G) Phalloidin labeled differentiating muscle cells in basal area of the coelomic epithelium. (H) Cell labeled with RN1 antibody (neuronal marker) in coelomic epithelia of the anlage. Red = DAPI stain, green D-F= HCR-FISH. G= Fluorescent Phalloidin, H= RN1 antibody. Bar- D-F= 25µm, G-H=10µm.

384

385 **C5 represents muscle precursors**. A second cell population known to originate from the coelomic epithelium and
386 that can be identified in our data is that of muscle precursors. These cells are known to differentiate into enteric
387 muscle during the second week of regeneration (Murray and García-Arrarás, 2004). This population can be
388 recognized in our data by the expression of muscle-specific markers present in C5, such as *TITIN*, *MYL1* (myosin
389 light chain 1/3), *MYH7* (myosin 7), *ACTG* (actin, cytoplasmic 2), and *CNN3* (calponin-3) (Fig 6A). Considering that
390 this cell population is potentially a population of the coelomic epithelium actively undergoing differentiation toward
391 muscle phenotype, they also share gene expression with other epithelial cell clusters (C0, C1, C3, C4), albeit at a
392 lower fold-change. Similarly, this cluster shows a specific expression of transcription factors associated to muscle
393 cells, namely *FXL16* (F-box/LRR-repeat protein 16) and *SCRT2* (transcriptional repressor scratch 2). Results of GO
394 terms of this cluster also demonstrate enriched terms related to muscle tissue growth, such as *muscle tissue*
395 *morphogenesis*, *muscle development*, *myofibril assembly*, and *sarcomere organization* (Fig 6B). The focus on
396 development and morphogenesis is to be expected, considering that these are still undergoing differentiation toward
397 a muscle phenotype. HCR-FISH of *MYH7* corroborates the muscle precursor phenotype of the cells in this cluster
398 (Fig 6D-F). Labeling is observed in the same regions as myoblasts or muscle cells were previously identified
399 (Murray and García-Arrarás, 2004), including differentiating muscle cells within or underlying the coelomic epithelia
400 of the mesentery and the anlage (Fig 6D & 6E) and, as expected, the muscle layer in the normal intestine (Fig 6F).
401 The same cell population found in the basal side of the coelomic epithelia of the regenerating intestine is labeled
402 with the muscle marker, fluorescently-labeled phalloidin as shown in Fig 6G.
403
404 **C9 represents the neuroepithelial cells.** Cells in C9, represent another population of specialized cells that can be
405 associated to cells previously described in the intestinal anlage. This small number (3%) of cells most likely
406 corresponds to neuroepithelial cells that will eventually give rise to neurons. These cells are shown to be expressing
407 neuroepithelial or neuronal genes such as neurotrypsin (*NETR*), potassium gated-voltage channels, *PRD10*
408 *(PRDM10* - PR domain zinc finger protein 10*)*, *ELAV2* and *STA10* (STARD10 - START domain-containing protein
409 10). The latter is a protein that we have characterized as being expressed by enteric neurons and nerve bundles
410 (Rosado-Olivieri et al., 2017) (Fig 6A). The holothurian STA10 (STARD10) is recognized by our monoclonal
411 antibody RN1. This antibody has been used to detect enteric neurons as they begin to differentiate in the coelomic
412 epithelium during the second week of regeneration (Tossas et al., 2014). Labeling of the 8-dpe regenerating

413 mesentery shows one of these RN1 neuronal cells in the coelomic epithelium of the regenerating anlage (Fig 6H).
414 Among its associated GO terms are *positive regulation of ion transmembrane transporter activity*, *cyclic nucleotide*
415 *metabolic process*, *regulation of muscle contraction, regulation of membrane potential* and *positive regulation of*
416 *hormone secretion* (Fig 6B). Moreover, there is also a great representation of processes involved in development,
417 differentiation, and growth of nerve cells, all of which together would be expected of a neuroepithelial layer.
418
419 The characterization of these 3 clusters, that represent cells undergoing differentiation or proliferation, leaves a
420 group of 4 clusters (C0, C1, C3, and C4) that show some overlap in expressed genes and at the same time share
421 some gene expression with some of the previously described clusters. Nonetheless, as seen in Fig 3A&B, the cells
422 in these four clusters still have high expression and representation of specific transcripts.
423
424 **C4 represents the intestinal coelomic epithelial cells.** The gene expression profile of cells in C4 sets them
425 slightly apart from the other three clusters (C0, C1, C3). It identifies cells that are more advanced in their
426 development toward a particular phenotype. C4 shows high expression of genes such *KCNQ5* (potassium voltage-
427 gated channel subfamily KQT member 5), *SC6A9* (sodium and chloride dependent glycine transporter 1), *EFNB2*
428 (Ephrin-B2), and *UNC5C* (Netrin receptor UNC5C) (Fig 7A). Other than these, C4 also shows high expression of
429 genes that are related to cell-cell interactions and ECM molecules such as *LAMA2* (laminin subunit alpha-2),
430 *MEGF6* (multiple epidermal growth factor-like domains protein 6), *FMN1* (formin-1), *NPHN* (nephrin). This cluster,
431 distinct from others, shows enrichment of GO terms related to more advanced stages of development, such as
432 *morphogenesis of epithelium*, *sensory perception*, *regulation of calcium ion transmembrane transport*, among others
433 (Fig 7B). Noteworthy, cells from this cluster correspond mostly to cell from the mesentery samples (67%) rather than
434 from the anlage (37%). Additionally, from all the mesentery cells, about 11% are part of this cluster, while only 4% of
435 the anlage cells are represented here. HCR-FISH of *SC6A5* (sodium- and chloride-dependent glycine transporter 2),
436 a gene differentially expressed in the cells of this cluster provided a surprising result. The expression of this mRNA
437 was observed in a few cells in the coelomic epithelia of the regenerating mesentery and intestinal anlage (Fig 7D-E).
438 However, intense labeling is observed in some cells of the normal intestine mesothelium. This pattern of labeling
439 strongly suggests that the labeled cells of the regenerating intestine grouped in C4 (both mesenteryal and anlage)
440 correspond to cells that are in a differentiation pathway to become part of the coelomic epithelia (possibly the

441 peritoneocytes) in the regenerated organ. This conclusion is strengthened by the pseudotime analyses presented in

442 the following section.

443

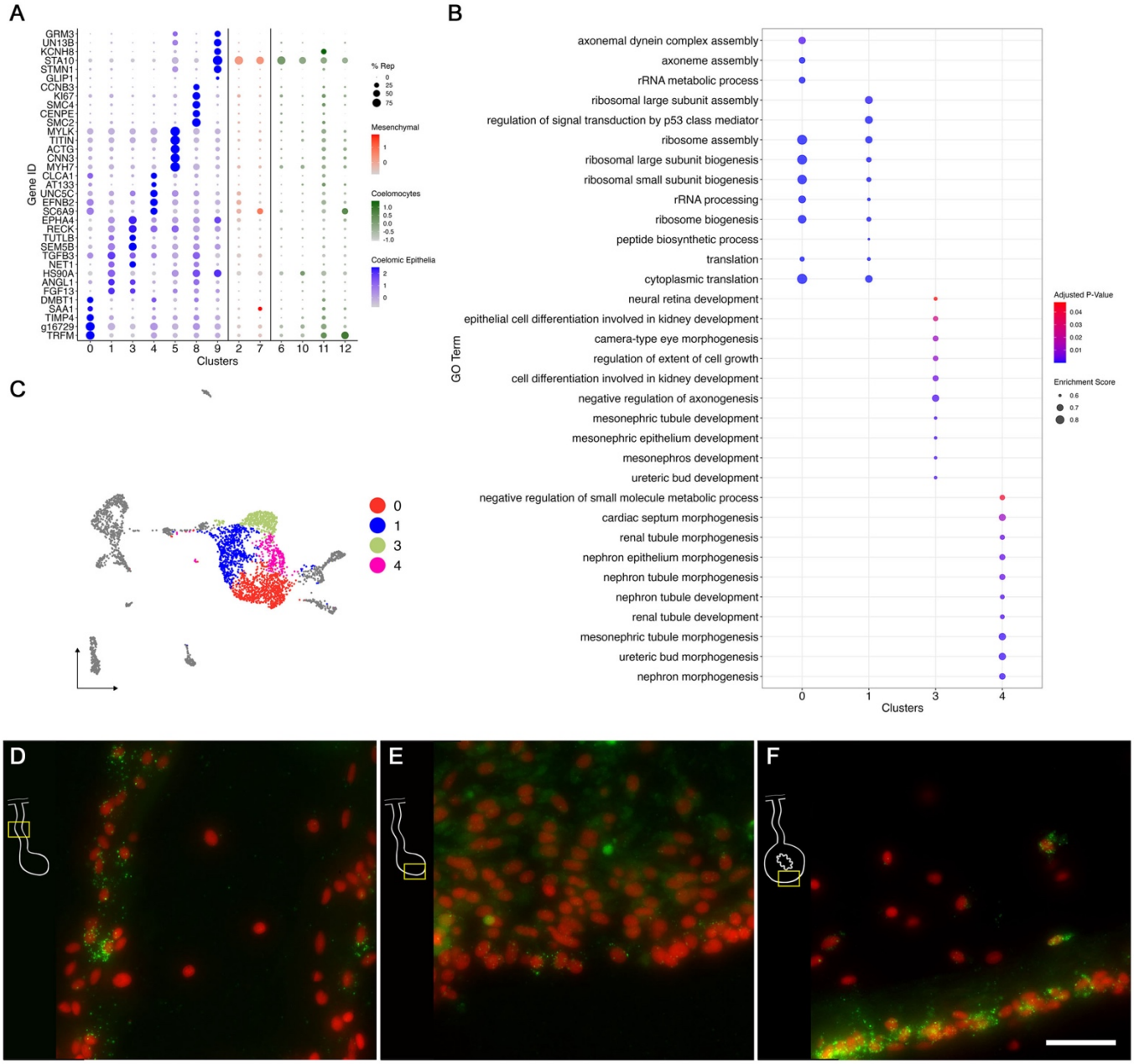

Fig 7. Expression profile of coelomic cell populations in the regenerating intestine anlage and mesentery. (A) Dot plot showing the top expressed genes of C0, C1, C3 and C4. Color intensity reflects expression levels in $\log_2$FC values. Dot size correspond to the percentage of representation of each gene in the respective cluster compared to all others. (B) Top GO enriched terms of biological processes of each cluster. Dot size corresponds to the enrichment score while the color reflects the adjusted p-value. (C) UMAP highlighting the clusters of the coelomic epithelial cells of the regenerating intestine. (D-E) HCR-FISH for *SC6A5* mRNA was performed as a marker for cells of C4. Labeling is observed in the (D) regenerating mesentery, (E) the coelomic epithelium of the anlage and (F) coelomic epithelium of the normal intestine. Red = DAPI stain, green = HCR-FISH. Bar= 25µm.

444

445 **C0, C1, and C3 represent differentiation stages of coelomic epithelial cells**. The three remaining clusters to be
446 analyzed are C0, C1, and C3. These three clusters share many of their top representative genes, which are
447 associated with developmental, regenerative, or oncogenic processes (Bradford et al., 2009; Dunn et al., 2006; Lu
448 et al., 2015; Nishimoto and Nishida, 2007; Oike et al., 2004; Zhao et al., 2008). These include, for cluster 0: *TRFM*
449 (melanotransferrin), *TIMP4* (metalloproteinase inhibitor 4), and *DMBT1* , for cluster 1: *FGF13* (fibroblast growth
450 factor 13), *TGFB3* (transforming growth factor beta 3), *HS90A* (heat shock protein HSP 90-alpha), and *ANGL1*
451 (angiopoietin-related protein 1) (Fig 7A), and for cluster 3: *SEM5B* (semaphoring-5B), *LRIG3* (leucine-rich repeats
452 and immunoglobulin-like domains protein 3), *TUTLB* (protein turtle homolog B), and *NET1* (netrin-1). Moreover, C0
453 and C1 share an over-representation of ribosomal genes (not shown), and this is reflected in their GO analyses that
454 highlights biological processes related to ribosomal activity such as *cytoplasmic translation*, and *ribosome assembly*,
455 *biogenesis*, and *assembly* (Fig 7B). In addition to these, C3 also showed enrichment of processes involved in the
456 development of tubular lumen-containing structures such as *mesonephric and ureteric ducts*, *differentiation and*
457 *regulation of cell growth*, and *negative regulation of axogenesis* (Fig 7B).
458
459 C1 and C3 are also closely related in their localization, being overwhelmingly associated with the anlage. These two
460 clusters are mostly composed of cells from the anlage tissue, where we expect to see the precursor cells that will
461 give rise to specialized cells of the organ (Fig 1D). Precisely, C1 and C3 cells together correspond to 37% of all
462 anlage cells, compared to 14.6% of all mesentery cells. In contrast, cells from C0 correspond to 27% and 18% of the
463 mesentery and anlage cells, respectively.
464
465 To obtain insight into these cell clusters, we performed HCR-FISH for two different mRNAs; *NET1*, a chemotropic
466 protein highly represented in C1 and C3, and *TRFM*, the top represented gene in C0. Both *in situ* hybridization
467 experiments labeled cells in the coelomic epithelium of the regenerating intestine, supporting our contention that the
468 large supra-cluster represents the coelomic epithelium layer. However, their spatial pattern of expression was
469 unpredictably different. While *NET1* was highly expressed in most of the coelomic epithelial cells of the anlage, little
470 expression was found in the regenerating mesentery or in the coelomic epithelium of the normal intestine (Fig 8G-
471 H). *TRFM*, in contrast, was highly expressed in the coelomic epithelium of the normal intestine and poorly expressed
472 in the intestinal anlage (Fig 8A-E). In the regenerating mesentery, a gradient in expression of the *TRFM* is observed,

473 where high levels of expression were found in the coelomic epithelium close to the body wall and diminished as one
474 approached the anlage. Thus, the HCR-FISH results show that C0, C1, and C3 correspond to cells of the coelomic
475 epithelium, but strongly suggest that C0 differs from C1 and C3 both in their gene expression profile and in the
476 localization where they are found, both in the regenerating and in the normal intestine.
477
478 Finally, it is essential to highlight the many signaling, or growth factors expressed by the coelomic epithelial clusters,
479 in particular C0, C1 and C3 (Fig 3). These include: Wnt, Hox, semaphorin, FGFs, TGF-beta, netrin, insulin-like
480 growth factor (IGF), growth/differentiation factors (GDF), and angiopoietin related proteins (ANGL) (e.g. *WNT9,*
481 *SEM5B, FGF13*, *NKx3.2*, *TGFB3*, *HOX9*, *IGF1*, *GDF8, ANGL1*, and *FOXF1*) (Fig 3). This is important in view that
482 the epithelium of the vertebrate blastema is characterized by its chemical modulation of the underlying
483 mesenchyme, as will be discussed later. Likewise, other genes that serve as markers of specific cell types or
484 cellular stages were also identified, including *PIWL1* (piwi-like protein 1) in C1, *YAP1* in C3 and C4, *HES1*
485 (transcription factor HES-1) in C1 and C3, and *PRRX1* (paired mesoderm homeobox protein) in C0 and C4 (Fig 3
486 and S5 Fig).
487
488 In summary, of the 13 clusters identified, our data strongly suggest that four of them (C9, C10, C11, and C12)
489 correspond to coelomocytes or immune cells, two of them (C2 and C7) correspond to cells with a mesenchymal
490 phenotype and the remaining 7 to cells of the coelomic epithelia. Of these seven, C5 corresponds to differentiating
491 muscle, C9 to differentiating neuroepithelium, C4 to differentiating coelomic epithelia and C8 to proliferating cells.
492 C1 and C3 represent most of the cells found in the coelomic epithelium of the anlage. In contrast, C0 represents a
493 coelomic epithelial phenotype more closely associated with the mesentery than the intestine.

494

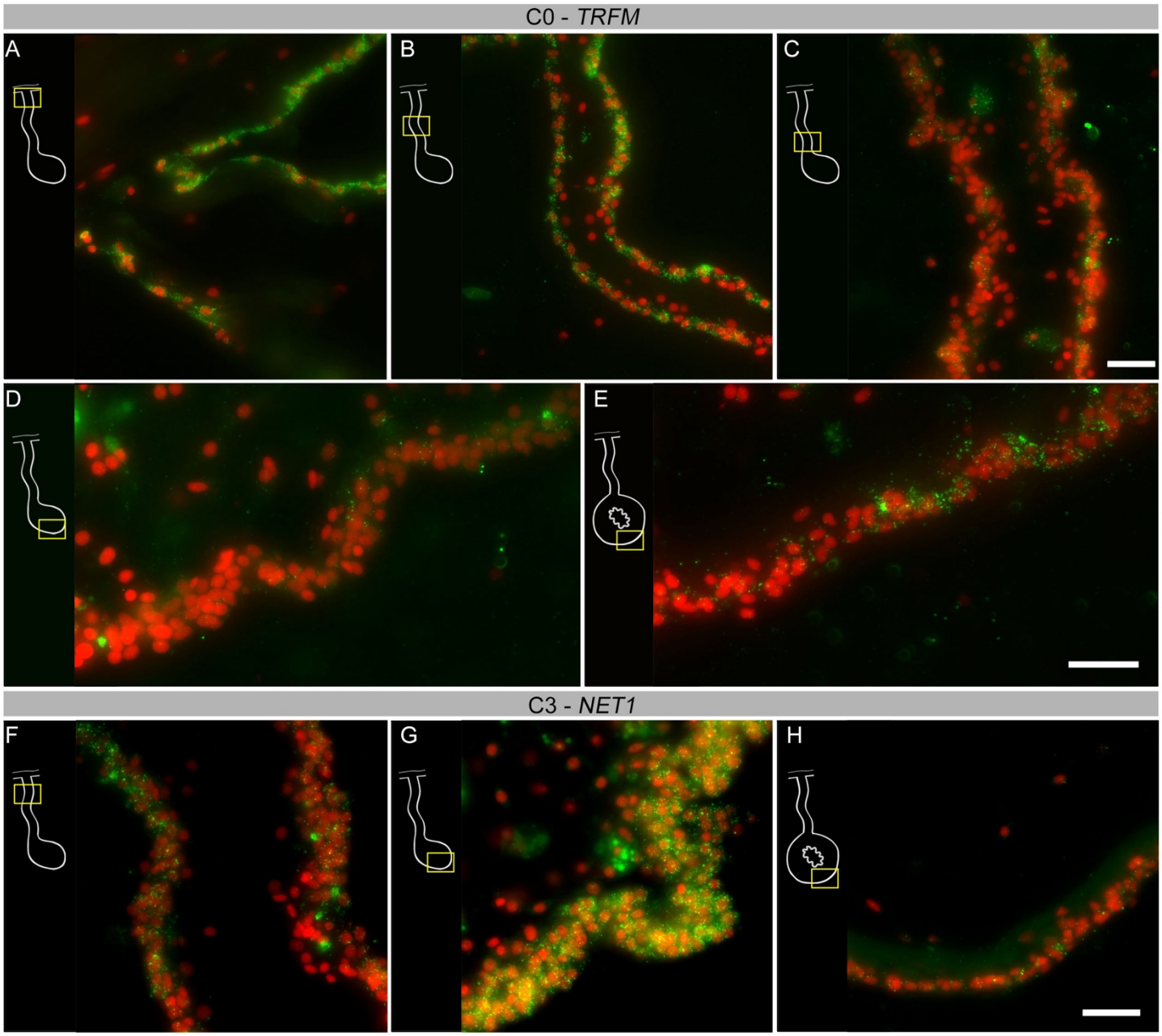

Fig 8. HCR-FISH for *TRFM and NET1* shows the differential gene expression of the anlage versus mesentery coelomic epithelia. *TRFM* is mainly expressed in the mesentery coelomic epithelial cells that are distant from the regenerating anlage while *NET1* is mainly expressed in the coelomic epithelial cells of the anlage *TRFM* mRNA expression (A-E) shows a gradient from (A) very strong expression in the coelomic epithelium at the attachment of the mesentery to the body wall, (B) high expression in the coelomic epithelia of the mesentery close to the body wall, (C) weaker expression in the mesentery close to the anlage to (D) weak or lack of expression in the coelomic epithelium of the anlage. (E) *TRFM* mRNA is expressed by the coelomic epithelium of the normal intestine. regenerating intestine. In contrast, few cells express (A) *NET1* mRNA in the regenerating mesentery, while high expression is found in (B) the coelomic epithelium of the anlage (C) Little expression of NET1 is present in the coelomic epithelium of the normal intestine. Red = DAPI stain, green = HCR-FISH. Bar= 25µm.

495 ## *Trajectory Analysis: What populations are driving cell specification?*

496

497 Among the many mysteries of the holothurian intestinal regeneration process is the identification of the precursor
498 cells. In simple terms, what are the cells from which all nascent cells derive from? We performed a trajectory
499 analysis of the data to provide some insights into this issue. This type of analysis is usually performed with samples
500 at different stages or time points. However, we considered it feasible to conduct this analysis because in the 9-dpe
501 regenerating anlage/mesentery we find cells at various stages of differentiation. These cells could provide crucial
502 information on how the cell populations are associated with each other. To address this, we initially employed RNA
503 velocity analysis. This method describes the temporal dynamics of gene expression based on the relative
504 abundances of spliced and unspliced mRNA across cell populations.

505

506 Our initial velocity analysis on all the clusters and samples (Fig 9A-B), provided three main results. First, the
507 direction of arrows in our UMAP shows them flowing towards C5, C9, and C4. These arrows do not point towards
508 any other cluster; thus, they are terminal arrows. Second, while arrows from C8 are not terminal, they are directed
509 towards C1. This suggests that cells in C1 provide cells for the growth of the anlage via proliferation. Thus, these
510 results support C5, C9 and C4 as terminal cell clusters which we have described as muscle, neuroepithelial, and the
511 nascent coelomic epithelium cells, respectively. Third, velocity embedding shows shorter arrows that point from
512 clusters 0 and 1 towards terminal populations previously described. Therefore, cells of C0 and C1 are not
513 undergoing significant transcriptional changes. The RNA velocity results of the rest of the clusters are less
514 interesting as they do not show directions towards any other clusters, mainly because of their individuality within the
515 UMAP. However, it is interesting that arrows of the mesenchymal cell populations show distinct directions and
516 lengths. Based on the results, it seems that portions of both mesenchymal clusters (C2 and C7) have gone or are
517 undergoing more extensive differentiation changes.

518

519 We then re-clustered C0, C1, and C3 cells, along with the differentiating cell populations (C4, C5, and C9) to better
520 understand their relationship (Fig 9C). The velocity assessment of these newly clustered populations resulted in a
521 similar pattern (Fig 9D). Here, we can see that the differentiating cells (C4, C5, and C9) have long arrows
522 suggesting that these cells are going through an advanced stage of transcriptional change compared to others
523 (Anderson et al., 2020; La Manno et al., 2018). It is clear from these results that C1 future states are cells of C3 and,

524 to some extent, C4. Moreover, it seems that C0 has a closer relationship to cells of C5 and C9 and that some cells
525 of these clusters could potentially differentiate into cells of C4 (the coelomic epithelium cells). In this case, to
526 complement and confirm our RNA velocity interpretation, we also performed a pseudotime analysis using Slingshot,
527 which relies on the expression data of each cluster. This analysis showed C1 in an earlier pseudotime than C3, C4
528 and C0 in the resulting two lineages (Fig 9D). The resulting lineages differed by the terminal clusters, one containing
529 C5 (muscle) and the other C9 (neuroepithelial). Thus, it supports what we have already visualized on the RNA
530 velocity embeddings.
531
532 The results described so far show that C0, C1 and C4 are cells in distinct differentiation states, but we wanted to
533 have a clearer view of the cell clusters that potentially have an essential role in the regeneration process. For this,
534 we made another subset of cells that corresponded to C0, C1, C3 and C4, but uniquely from cells of the anlage (Fig
535 9F). The rationale was that cells from the mesentery are certainly at a different state from those of the anlage and
536 thus could interfere with the pseudotime of cells from the anlage. The RNA velocity analysis using this subset
537 strengthened our previous inferences. First, C1 seems to be the least dedifferentiated cell cluster, whose future
538 state will be cells of C3 and part of the population of C4. Second, that C0 seems to be in a specialized state of
539 differentiation that has a relationship to C4 (Fig 9G). This would explain the relationship of this cluster to that of the
540 differentiating cells of C5 and C9. Interestingly, portions of C1, C0 and C4 appear to be in an advance process of
541 differentiation based on their longer arrows compared to C3 and another portion of C4 close to C3 (Fig 9G). The
542 Slingshot analysis of the anlage cells from C0, C1, C3 and C4 revealed that the pseudotime starts at a point of
543 convergence that contains a portion of cells from C1 and C0. Yet, it further supports the cells from C1 as the least
544 differentiated (Fig 9H). C1 is then followed by cells of C3, C4 and lastly C0, which for the most part seems to be at a
545 more advanced differentiation state with a closer relationship to differentiating cells (Fig 9I).
546

547

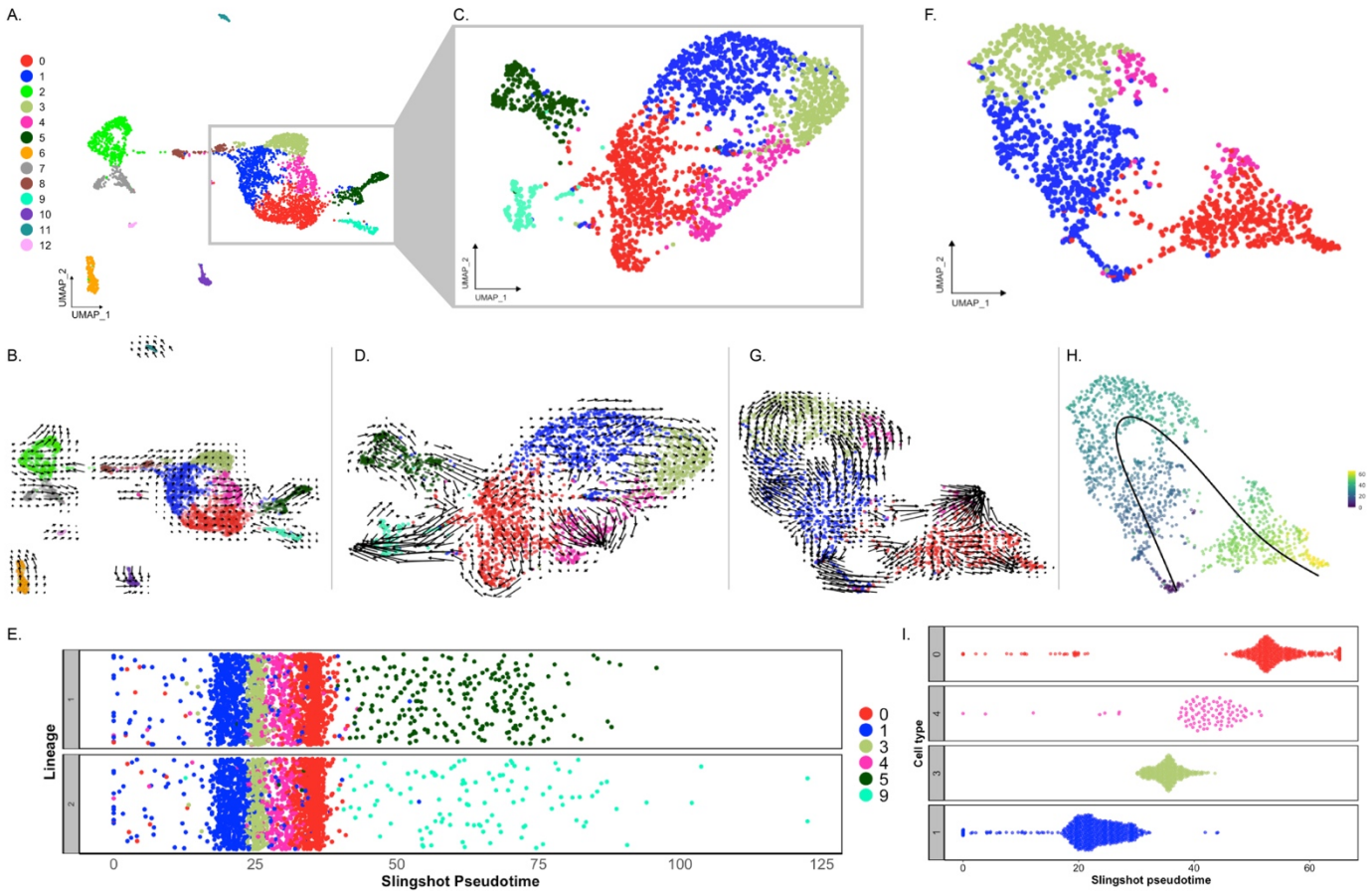

Fig 9. Trajectory analysis of cell populations from the regenerating intestinal tissue. (A) UMAP plot of all identified clusters. (B) RNA velocity embedded in UMAP of all main clusters. (C) UMAP of re-clustering of cells from C0, C1, C3, C4, C5, and C9. (D) RNA velocity analysis results from the subset from panel (C). (E) Jitter plot of Slingshot pseudotime of cells from C0, C1, C3, C4, C5 and C9. Pseudotime resulted in two lineages one containing C5 and the other C 9. (F) UMAP of re-clustered anlage cells corresponding to C0, C1, C3, and C4(G) RNA velocity results from the cluster results from panel F. (H) UMAP of panel F plot overlayed with pseudotime results of Slingshot. Color represent pseudotime values from 0 (blue) to 60 (yellow). (I) Jitter plot showing the Slingshot pseudotiume of cells from each cell cluster.

548

Discussion

In this study we employed scRNA seq and HCR-FISH techniques to examine the cellular phenotypes in regenerating intestinal tissues of the sea cucumber *H. glaberrima*. These techniques have been seldom used to characterize echinoderm cells, and the few studies available are mainly limited to embryonic stages of sea urchins (*Strongylocentrotus purpuratus, Lytechinus variegatus)* and the sea stars (*Patiria miniata)* (Cocurullo et al., 2023; Foster et al., 2022; Meyer et al., 2023; Paganos et al., 2022a, 2022b, 2021; Tominaga et al., 2023). Nonetheless, these studies provide an excellent description of the cell population and dynamics arising from major germ lines during echinoderm development. We now apply the same techniques to explore cell phenotypes involved in intestinal regeneration in holothurians. This is, to our knowledge, the first-time scRNA-seq and HCR-FISH have been used in adult echinoderms to analyze the cellular and molecular basis of their amazing regenerative properties. This research integrates the extensive cellular and molecular information on intestinal regeneration in holothurians collected over the past two decades, offering a comprehensive view of the cellular phenotypes and molecular changes involved.

Cell types and differentiation stages in the 9-dpe regenerating intestine.

Our study has focused on the description of cells present in the 9-dpe regenerating intestine of the sea cucumber, where cells are known to have gone through dedifferentiation and are, at this time-point, in the process of differentiating into specialized cells (García-Arrarás et al., 2011). Based on our analysis we have identified 13 distinct populations that form part of the regenerating intestinal mesentery and anlage (Fig 1B). Among these clusters we have described the clusters corresponding to the coelomocyte, coelomic epithelium, and mesenchyme cell types (Fig 3). Thus, we can now use the information that our laboratory and others have gathered to pinpoint the cellular mediators and their activity during regeneration. The coelomic epithelia, for example, is highly influential in the regeneration process as it is the site where major cellular events occur, particularly cell division, dedifferentiation, and differentiation (García-Arrarás et al., 2011). Moreover, the mesenchyme ECM is known to undergo remodeling during the regeneration process, which is also critical for the proper growth of the new tissue (Quiñones et al., 2002). However, while much of the events have been described using microscopic and histological

577 tools, we need a more comprehensive understanding of the transcriptomic characteristics of specific cell populations
578 involved in the regeneration process.
579

580 *The sea cucumber contains various mesenchymal and coelomocyte populations*
581
582 Amongst the phenotypes identified are clusters of mesenchymal (C2 and C7) and coelomocyte cell populations (C6,
583 C10, C11, and C12). The mesenchymal populations demonstrated a unique expression of *ERG* and *ETS-1*, markers
584 of mesenchymal populations in other echinoderms. *ETS-1* has long been associated with developmental processes
585 of mesenchymal formation in sea urchin (Koga et al., 2010; Rizzo et al., 2006). In other studies, *ERG*, a member of
586 the ETS gene families, has been found to be necessary for controlling mesenchymal identity and differentiation (Cox
587 et al., 2014; Mochmann et al., 2013). Further analyses of their individual marker genes suggest that these cells
588 might be involved in EMT. For instance, C2 expresses *TIMP3*, a metalloproteinase inhibitor that aids in the
589 extracellular matrix remodeling (Dewing et al., 2020), and *NPNT*, a gene reported to be related to development and
590 cancer processes (Magnussen et al., 2021). These genes are also crucial for cells undergoing EMT as the cells
591 need to detach from the other cells and the basal lamina that forms the epithelium. Comparatively, the expression
592 profile of C7 with genes such as *PA21B* (phospholipase A2), *TMPS9* (transmembrane protease serine 9), *SEPP1*,
593 *DMBT1*, *ITIH3*, and *SVPE1* and its GO results suggest this mesenchymal population is undergoing different
594 processes. Based on these contrasting expression profiles, we propose that C2 corresponds to cells that have
595 recently undergone EMT from the coelomic epithelium and eventually differentiate into a more specialized
596 phenotype (C7). Our pseudotime results further support this developmental transition as cells in C7 appears to be in
597 a more advanced stage when compared to those of C2 (S6 Fig). Therefore, these two populations correspond to the
598 first transcriptomic description of mesenchymal phenotypes reported in sea cucumber regenerating intestine.
599

600 Our dataset contains four distinct populations that we have characterized as coelomocytes. The coelomocyte
601 populations reported in different holothuroid species ranged between 4 to 6 distinct types (Hetzel, 1963; Ramírez-
602 Gómez et al., 2010; Xing et al., 2008). Studies from our laboratory previously revealed four different coelomocyte
603 populations in *H. glaberrima,* distinguished by their morphology, histochemistry, and phagocytic activity. These were
604 lymphocytes, phagocytes, spherulocytes and a population named “giant cells” (Ramírez-Gómez et al., 2010). The

605 distinctive gene expression profile of each of the coelomocytes that we have identified can provide insights into the
606 differences in their role as immune/circulating cells within the sea cucumber. For example, the C6 marker gene
607 fibrinogen-like protein, which is part of a protein family known as FREP, makes this population of great interest.
608 Mainly because these molecules have been vastly studied across invertebrates, and multiple immune roles have
609 been proposed, including phagocyte recognition and encapsulation (Hanington and Zhang, 2011). A distinct
610 example is that of C10, where the expression of *HCK*, *FER* and *ITF8* markers suggest this might be a macrophage-
611 like activity (Chen et al., 2023; Dolgachev et al., 2018; Shuttleworth, 2018). Specifically, *HCK*, a member of Src
612 family kinases (SFK), has been closely related to macrophage activation and polarization (Bhattacharjee et al.,
613 2011; Poh et al., 2015). Interestingly, recent studies in *A. japonicus* found that an Src homolog mediates the
614 phagocytosis of *Vibrio splendidus,* which further supports C10 immune identity (Wan et al., 2022). Thus, to our
615 knowledge, this would be the first report of the expression profile of distinct coelomocyte populations in an adult
616 echinoderm species, setting up the stage for integrating these populations with the previously described ones.
617

618 ### *The coelomic epithelia of the intestinal anlage is composed of a heterogenous population of cells*

619
620 Our research findings align with previous microscopic descriptions of cells in the normal and regenerating
621 mesothelium and coelomic epithelia. In our data, we most easily identify the cell population that forms the cluster
622 exhibiting a proliferative phenotype (C8). Proliferative cells in the regenerating intestine are primarily localized within
623 the coelomic epithelium of the anlage (García-Arrarás et al., 2011, 1998; Reyes-Rivera et al., 2024), and the gene
624 expression profile documented here unequivocally identifies these as proliferative.
625

626 A second population of cells that can be well correlated to previously described cells is that with a muscle cell
627 phenotype (C5). The evidence suggests that this cell population represents those cells from the coelomic epithelium
628 that are differentiating into myocytes. This evidence includes: (1) the top-expressed genes by the cells in this
629 cluster are all muscle-associated genes; (2) the top-enriched terms are all related to muscle morphogenesis; (3) the
630 cluster is mostly composed of cells that come from the anlage where muscle formation is known to be taking place
631 at this stage (Murray and García-Arrarás, 2004); (4) differentiated muscle cells were not dissociated by the
632 enzymatic procedure strongly suggesting that the muscle cells that we have identified in our data are those that are

633 in a differentiation process, rather than fully differentiated cells closer to the body wall; (5) the cells in this cluster
634 were identified by HCR-FISH of *MYH7.* These cells are localized toward the basal region of the coelomic
635 epithelium, the region where the differentiating myocytes are known to be present (Murray and García-Arrarás,
636 2004). Moreover, among the top expressed genes of this cluster is Troponin I (*TNNI1*), which has also been
637 reported to be highly expressed in muscle precursor cells of the sea star embryo and immature cardiomyocytes of
638 the chicken (Mantri et al., 2021; Tominaga et al., 2023). The high differentiation activity of these cells is also
639 supported by our pseudotime analysis, where distinct cells within the cluster are in individual differentiation states
640 (Fig 9D&E). Further analysis of these populations could allow us to understand the transcriptional changes these
641 cells undergo to become fully specialized muscle cells.
642
643 An additional population in our dataset, is the neuroepithelial population (C9). This population has *STARD10*,
644 among its top expressed genes, known to be a phospholipid transfer protein present in a neural cell population
645 localized in the coelomic epithelium of the intestine (García-Arrarás et al., 2019; Rosado-Olivieri et al., 2017).
646 Furthermore, cells of this cluster have high expression of other genes reported to be expressed by neuronal cells of
647 regenerative and developmental tissues, such as beta-tubulin in developing human gut and sea urchin larva, and
648 synapsin in planaria regenerating tissue (Cocurullo et al., 2023; Elmentaite et al., 2020; King et al., 2024).
649 Interestingly, an earlier study showing that beta-tubulin positive cells arise from dedifferentiated cells of the
650 regenerating intestinal tissue of the sea cucumber (García-Arrarás et al., 2019) also suggests that similar to the
651 muscle population, these cells are neuroepithelial cells that are differentiating rather than fully specialized. Further
652 support for this theory lies in the main contribution to C9 coming from anlage cells and their terminal differentiation
653 state observed in the pseudotime analysis (Fig 1D & 10D).
654
655 The remaining four clusters of the coelomic epithelium supra-cluster are more challenging to characterize.
656 Nonetheless we will explore some hypotheses regarding their cellular phenotypes. The identity of C4 was put
657 forward based on its close transcriptional and pseudotime correlation with populations of the coelomic epithelia (Figs
658 3 and 9). Additionally, in our *in situ* hybridization, its marker gene *SC6A5*, is mainly expressed by the coelomic
659 epithelial cells of the normal intestine, strongly suggesting that the cells expressing this gene in the anlage are those
660 that will become the coelomic epithelial cells of the regenerated organ (Fig 7).

661

662 C0 remains an intriguing cell population. On one hand it appears to be closely related, by its gene expression, to
663 other coelomic epithelial populations (Fig 3). Thus, it may represent an unknown cell population or cell stage. The *in*
664 *situ* expression suggest that this cluster represents the cellular population of the mesentery or peritoneal coelomic
665 epithelium. In this case we might be evidencing differences in the coelomic epithelium of the mesentery (exemplified
666 by cluster 0) from those of the coelomic epithelium of the intestine (exemplified by cluster 4). Future experiments will
667 be needed to address this controversy.

668

669 Lastly, C1 and C3 share many common genes, and represent distinct populations but are still closely associated,
670 regardless of the clustering parameters or the statistical assessment performed. Although we considered combining
671 them into a single cluster, we ultimately decided against it, as they likely represent different stages of cell
672 development or plasticity in the regenerating intestine. One-to-one comparisons revealed that C1 expressed various
673 ribosomal gene markers, while C3 expressed specific genes such as *EPHA4* (ephrin type-A receptor 4) and *LRIG3,*
674 indicating distinct transcriptomic states. Additionally, all trajectory analyses revealed that C1 cells appear to give rise
675 to C3 cells.

676

677 Further characterization of the least differentiated cells, C1 and C3, within the anlage coelomic epithelium suggest
678 that these cells probably serve as cellular precursors to differentiating cells. The evidence from pseudotime
679 analyses and gene expression of C1 and C3 strongly support this conclusion. These cells appear to exhibit
680 pluripotency with the potential to form muscle, neurons, coelomic epithelia and mesenchymal cells in the
681 regenerating intestine. Their gene expression profiles include markers from gene families associated with embryonic
682 development such as Hox, zinc fingers, basic helix-loop-helix and others, some of which are linked to stemness and
683 pluripotency. For example, *HSP90A*, a molecular chaperone essential for stem cell pluripotency, and markers like
684 *HES1* and TGFb, essential for maintaining stem cell proliferation, are present in these cell populations (Aztekin,
685 2021; Mishra et al., 2005). Moreover, the expression of *PIWL1* (piwi-like protein 1) and *YAP1* further support the
686 classification of these clusters as precursor cells of the intestinal anlage. In hydra, piwi-like molecules are
687 exclusively localized in stem/progenitor cells (Juliano et al., 2014), and in mice, *YAP1* is expressed only in
688 multipotent cells during intestinal epithelium regeneration, vital for their emergence (Ayyaz et al., 2019). Ultimately,

689 trajectory analysis also supports C1 as a precursor cell population, as the dividing cells (C8) appear to give rise to
690 C1, which then progresses toward C3. This analysis aligns with evidence of a proliferation center in the coelomic
691 epithelia that provides precursor cells essential for the growth of the anlage.
692
693 C1 and C3 cells are probably dedifferentiated cells from the mesentery mesothelium, retaining markers common to
694 all epithelial cells. Similar to what is known in other highly regenerative organisms, these dedifferentiated cells can
695 proliferate and then re-differentiate into the cells of the new organ. Future experiments will determine whether they
696 retain the memory of their previous phenotype (muscle or coelomic epithelium) or are completely pluripotent.
697

698 *The coelomic epithelium of the intestinal anlage is pluripotent*

699
700 Regardless of which cell population is responsible for giving rise to the cells of the regenerating intestine, our study
701 reveals that the coelomic epithelium, as a tissue layer, is pluripotent. Thus, it is capable of giving rise to various cell
702 types. Microscopy studies across different echinoderm species have consistently suggested that the coelomic
703 epithelium can differentiate into various cell types. Among these are the formation of muscle cells and neurons in
704 sea cucumbers (Yu Dolmatov et al., 1996), mesenchymal cells in brittle star (Piovani et al., 2021), and even immune
705 cells (coelomocytes) in sea star (Byrne et al., 2020; Sharlaimova et al., 2021). In some species, the coelomic
706 epithelium has even been proposed to transdifferentiate into intestinal luminal cells (Mashanov et al., 2005).
707
708 The direct association of pluripotency with the coelomic epithelium is evident in both the homeostatic regenerative
709 processes that maintain cellular numbers and in the regenerative responses to injury or autotomy. In some cases,
710 pluripotency is directly associated with the coelomic epithelium of the regeneration anlage. This is exemplified in the
711 brittle star *Marthasterias glacialis,* where it has been suggested that the coelomic epithelium is not only involved in
712 arm regeneration but also serves as a source of immune cells (Guatelli et al., 2022). This report indicated that
713 “residential stem cells” in the regenerating arm of the brittle star originate from the coelomic epithelia (Candia-
714 Carnevali et al., 2009). Similarly, in the sea cucumber *Holothuria forskali*, the injured mesothelial layer has been
715 identified as the source of undifferentiated cells that differentiate into the cells of the growing organ and into
716 phagocytic cells, now recognized as coelomocytes (Vandenspiegel et al., 2000).

717

718 Our scRNA-seq provides convincing evidence that various cell populations originate from the coelomic epithelia of
719 the sea cucumber anlage, offering a more detailed view of the differentiation process. These cell populations, now
720 classified by their gene expression data, correlate well with those previously characterized by microscopy
721 descriptions. We have strong evidence for muscular, proliferating and neuroepithelial cells (C5, C8, and C9) arising
722 from the coelomic epithelia of the anlage. We also show evidence of a differentiating cell population corresponding
723 to the mature intestine coelomic epithelium (C4). Furthermore, our data suggest the presence of a mesenchymal
724 population arising from the coelomic epithelium of the anlage through EMT (García-Arrarás et al., 2011).

725

726 Of particular interest, our study reveals that the mesentery coelomic epithelia population (C0) exhibits localized
727 expression of *SAA1*, an immune response related gene. This finding, in line with previous reports of SAA1
728 localization in the coelomic epithelium of the regenerating intestinal tissue (Santiago et al., 2000) (S5 Fig), raises the
729 intriguing possibility that the coelomic epithelium of the sea cucumber regenerating intestine could also be the
730 source of coelomocytes, as suggested by Guatelli (2022) (Guatelli et al., 2022). This hypothesis is further supported
731 by the observation that in the sea star *Asteria rubens,* coelomocytes arise from its coelomic epithelium (Vanden
732 Bossche and Jangoux, 19976). However, our current results, while suggestive, do not yet provide conclusive
733 evidence to support this in the sea cucumber, at least not in the coelomic epithelia of the regenerating intestine or
734 the 9-dpe stage.

735

736 Currently, there is no definitive evidence identifying the precursor cells that give rise to these cell populations in
737 echinoderms. However, given our gene expression data and the interactions observed among the cell populations,
738 we postulate that cells from C1 stand as the precursor cell population from which the rest of the cells in the coelomic
739 epithelium arise. Granted, much more experimental evidence will be needed to arrive at this conclusion.
740 Nonetheless, it provides a focus on the most likely, and probably most intriguing cell population. It also provides the
741 path to explore multiple questions that arise from our results. Can C1 be subdivided into other cell populations? Are
742 the cells in this cluster pluripotent? Do these cells originate from the same cells via dedifferentiation? These and
743 many other questions will indeed be tested in future experiments.

744

745 Our data has allowed us to construct a model of the cell populations we identified in the 9-dpe intestinal anlage (Fig
746 10). This model presents the coelomic epithelium of the anlage as a heterogeneous layer of cells comprising of six
747 cell populations corresponding to distinct differentiation states. Among these are cell populations in the process of
748 differentiation: muscle, neuroepithelium, and coelomic epithelium cells. We also propose the presence of
749 undifferentiated and proliferating cell populations in the coelomic epithelia, which give rise to the cells in this layer.
750 Underneath the coelomic epithelia are the mesenchymal cells, some of which may have originated from the
751 coelomic epithelial layer via EMT. Not shown in our model is a population localized in the coelomic epithelium of the
752 mesentery that we infer also plays an important role in the regeneration process of the intestine.

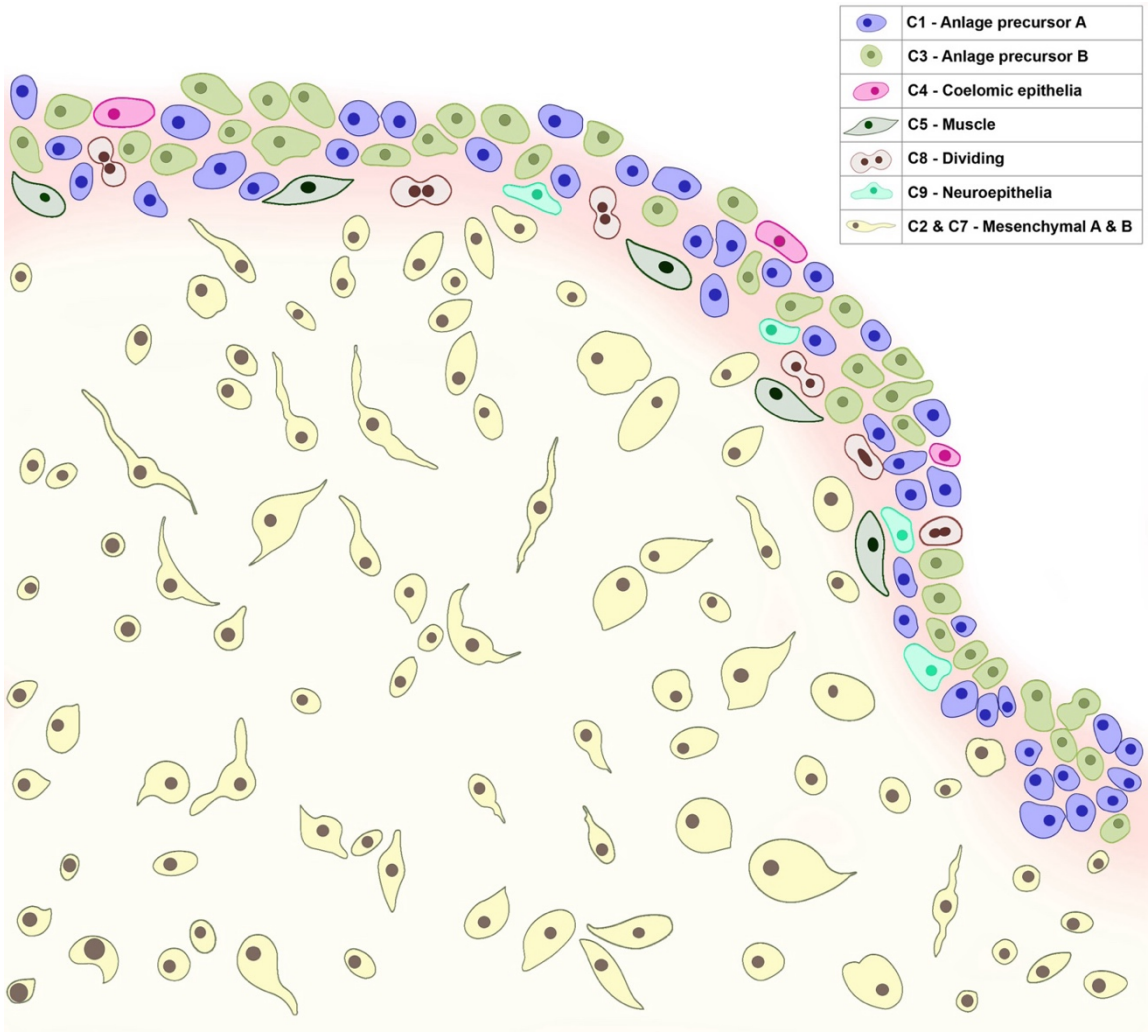

Fig 10. Model of cellular organization within the anlage of the regenerating intestine of the sea cucumber *H. glaberrima* at 9 dpe. Schematic highlights the heterogeneity of the coelomic epithelia of the intestinal anlage and identified mesenchymal populations. The colors of cells and C# correlate with those used on the UMAP of Fig 1B.

753

754 ## *The intestinal anlage as a regeneration blastema*

755

756 The intestinal anlage is a particular regenerative structure that has long been described as a blastema-like structure
757 due to its remarkable morphological resemblance to the “classical blastema” (García-Arrarás et al., 1998). As stated
758 previously a blastema is usually described as a transient structure composed of a mass of proliferating
759 undifferentiated cells. This structure is found at the site of injury and will give rise to the regenerated organ (Seifert
760 and Muneoka, 2018). The blastema cells can originate from different lineages across species. For example, in
761 amphibians, the blastemal cells originate from dedifferentiated muscle, cartilage, fibroblast and other tissues, while
762 in the flatworm they originate from undifferentiated stem cells known as neoblasts (Baguñà, 2012; Globus et al.,
763 1980; Wagner et al., 2011). The blastema is overlayed by a wound epidermis that is formed by a re-epithelization
764 process following injury, which develops into a specialized wound epidermis that in amphibians is known as the
765 apical epithelial cap (AEC) (Aztekin, 2021). Since its first description, more than 100 years ago, the blastema has
766 been regarded as the best indicator of regeneration, and its presence is associated with tissues or organs that are
767 highly regenerative. In fact, it has been proposed that the presence or absence of a blastema defines the
768 regenerative success or failure of the regeneration process. However, as more regenerative species continue to be
769 studied, the classical definition of a blastema has been reconsidered, moving towards its functional role rather than
770 its histological or structural characteristics (Seifert and Muneoka, 2018).

771

772 The blastema of salamanders and newts, have long served as models to describe a blastema cellular and molecular
773 properties (Globus et al., 1980; Scimone et al., 2022; Tajer et al., 2023). The sea cucumber intestinal anlage stands
774 as a different structure in terms of the tissue compartmentalization of certain activities. Yet, when examined closely,
775 much of the processes and signaling molecules described in the amphibian blastema also take place in the
776 holothurian anlage, although their spatial occurrence might differ. For instance, like the blastema cells of the
777 amphibians, the cells of the holothurian anlage coelomic epithelium are proliferative undifferentiated cells and
778 originated via a dedifferentiation process. Moreover, some of the genes expressed by the amphibian blastema cells
779 or the overlying AEC, such as Wnt, Tgf-beta, and Fgf, are also known to be expressed during sea cucumber
780 regeneration (Auger et al., 2023; Zeng et al., 2023). In amphibians, some of these factors are thought to be released
781 by cells of the AEC, serving as a way of modulating the blastema cell activity. For example, FGF1 is expressed in

782 the cells of the AEC while FGF receptors were localized to blastema cells(Zenjari et al., 1996). Moreover, both FGF
783 and Wnt signaling have been shown to be vital for the formation of the blastema (Makanae et al., 2014).
784
785 This expression of Fgf and Wnt and their possible functions correlates with what has been found in sea cucumbers.
786 Not only are the same growth factors expressed in C1 and C3, but a recent study highlighted the role of *FGF4* as a
787 modulator of cell proliferation during the intestinal regeneration of the sea cucumber *A. japonicus* (Zeng et al.,
788 2023). This group demonstrated that inhibiting *FGF4* and its receptor, *FGFR2,* negatively affected cell proliferation
789 of the mesothelial layer during intestinal regeneration. Similar results have been shown for Wnt, primarily a study by
790 our laboratory demonstrating that Wnt pathway inhibition, either by pharmacological drugs or by RNAi caused a
791 reduction in cell proliferation (Alicea-Delgado and García-Arrarás, 2021; Bello et al., 2020). Thus, in the sea
792 cucumber coelomic epithelia of the anlage, cells are also involved in intercellular communications that modulate
793 cellular dynamics through factors similar to those found in the AEC-blastema cell modulation.
794
795 The holothurian anlage and the amphibian blastema exhibit some differences. In the latter there is a clear
796 separation of the AEC and the underlying blastema cells. In amphibians, the AEC has been shown to actively
797 participate in the formation and maintenance of the blastemal cells, particularly in their proliferation and
798 differentiation. In contrast, in holothurians, cells with both blastema and AEC characteristics can be found within the
799 coelomic epithelium. In fact, both *PRRX1* (paired mesoderm homeobox protein), a gene expressed by amphibian
800 blastema cell precursors (Gerber et al., 2018; Lin et al., 2021), and *HES1* (transcription factor HES-1), a marker
801 gene of the amphibian AEC, are expressed by the holothurian coelomic epithelium (Aztekin, 2021) (Fig 3 and S5
802 Fig).
803
804 In conclusion, in all cases where it has been studied, the blastema appears as a dynamic structure where
805 communication among its cells and the overlying epidermis or epithelium plays important roles in the regenerative
806 process. In this context, the sea cucumber intestinal anlage could be considered a blastema since it uses similar
807 mechanisms to fulfills the same role in the regeneration of the new organ. In this case, the cells of the coelomic
808 epithelium would be those considered to be the blastemal cells.
809

Methods

Animals and Sample Collection

Two adult sea cucumbers were collected from the northeastern rocky region of Puerto Rico and were kept in aerated sea water for acclimatation prior to experiments. Evisceration of the sea cucumber was stimulated by intracoelomic injection of 0.35 M KCl as previously described (Reyes-Rivera et al., 2024). They were maintained in sea water aquaria for 9 days to undergo regeneration until dissection. Before the dissection, animals were anesthetized by immersion in ice-cold water for 45 minutes. Dissection was done through an initial dorsal incision which allowed exposition of the internal organs, upon which the growing rudiment (or anlage) and mesentery were dissected and separated from each other. Each tissue was kept in CMFSS on ice and treated separately during the tissue dissociation process.

Tissue Dissociation

Mesentery and rudiment tissues were digested for 15 minutes, in rocking shaker at room temperature with 1mL of 0.05% Trypsin/0.02% EDTA solution prepared in CMFSS (Bello et al., 2015). Digestions were quenched by adding 500μL of 0.2% BSA in CMFSS and then centrifuged for 2 minutes at 1500 rpm. The supernatants were discarded, and the pellets resuspended with 500μL of 0.04% BSA in CMFSS and the cells were gently separated by pipetting using glass pipets with fire blunted tips. The cell suspensions were filtered using a nylon cell strainer with 70mm mesh and aliquots were taken for cell counting. Cell viability was assessed through manual cell counting with hemocytometer to confirm that a viability higher than 90% was maintained. Sample suspensions were adjusted to 1000 cells/mL using CMFSS, as required for sequencing procedures.

Immuno- and cytochemistry

Fifty μL of dissociated cell sample were placed on polysine-treated slides and fixed with 50 μL of 4% paraformaldehyde and left to dry overnight. Slides were washed in PBS prior to use for immune and or cytochemistry. The methodology for the immunofluorescence techniques/preparation of slides was followed as

published except for the time of PBS washes which were of 10 minutes instead of 15 minutes (Diaz-Balzac et al., 2007; Reyes-Rivera et al., 2024). The primary and secondary antibodies used are in S7 Table. Samples to be probed with fluorescent phalloidin were treated directly with Phalloidin-TRITC (1:1000; Sigma P1951) for 1h as described previously (Reyes-Rivera et al., 2024). DAPI was incorporated into the mounting medium as described previously (Reyes-Rivera et al., 2024). Cells were observed in a Nikon DS-Qi2 fluorescent microscope.

Single Cell RNA Sequencing and Data Analysis

Single cell libraries were prepared using the 10X Genomics Chromium Next GEM Single Cell 3' Kit v3.1 and the Chromium 10X instrument, following the protocol from manufacturer (CG000204). Sequencing was carried out with Illumina NextSeq 2000 at the Sequencing and Genotyping Facility of the University of Puerto Rico Molecular Science Building.

The raw sequencing reads from all four samples (two mesentery and two anlage) were processed individually using Cell Ranger (v7.1.0) (Zheng et al., 2017) using the reference genome and gene models of *H. glaberrima* available at blastkit.hpcf.upr.edu/hglaberrima-v1. Gene models were annotated against human reference proteins from Uniprot and the entire Uniprot reference protein database. Gene IDs throughout the study correspond to the annotations with the human reference protein sequences from Unitprot.

Initial quality control was conducted in R (v4.3.2) using SoupX (v1.6.2) with default parameters to remove ambient RNA (Young and Behjati, 2020). Subsequent data processing was carried out using Seurat (v4.3.0.1) (Hao et al., 2024, 2021; Satija et al., 2015; Stuart et al., 2019). After data normalization and identifying variable features (n=2000), 22,970 anchors were identified using 20 dimensions. The datasets were integrated using the canonical correlation analysis (CCA) approach of Seurat, followed by data scaling for principal component analysis (PCA) (npcs = 50) and Uniform Manifold Approximation and Projection (UMAP) dimensional reduction technique (dims = 1:20).

866 Neighbors were then identified with 20 dimensions, leading to cluster identification at a resolution of 0.5. Various
867 resolution parameters (0.8, 1.2, and 1.4) and dimensions (up to 35 in increments of 5) were tested before the final
868 resolution value. The statistical analysis tool scSHC was employed to assess the probability of each cluster being
869 unique (Grabski et al., 2023). Marker genes of each cluster or supra-clusters were identified using the FindMarkers()
870 function in Seurat and mapped to the appropriate Uniprot IDs. Genes highlighted throughout the study where further
871 validated using the NCBI non-redundant reference database and EchinoBase (Telmer et al., 2024) via BLAST.
872
873 Differential expression data across clusters was used to perform gene set enrichment analysis of Gene Ontology
874 (gseGO) biological processes terms using clusterProfiler (v.10.0) (Yu et al., 2012) with a p-value cutoff of 0.05. For
875 this analysis, BLASTp was used to map *H. glaberrima* gene models to human reference protein sequences from
876 NCBI (GCF_000001405.40), facilitating the assignment of ENTREZ ID to the correct human GO terms in the
877 AnnotationDbi (v1.64.1) human database (v2.1) (Pagès et al., 2024).
878
879 RNA velocity loom files were generated with velocyto (v0.17), which relied on genome-masked regions obtained
880 from RepeatModeler (v2.0.5) and RepeatMasker (v4.1.5) (Smit et al., 2015; Smit and Hubley, 2015), along with the
881 sea cucumber gene models and CellRanger dataset. These files were further analyzed with velocyto.R (v0.6) and
882 SeuratWrappers (v0.2.0), using the ReadVelocity and RunVelocity functions. Pseudotime analysis for the distinct
883 data subsets was conducted using Slingshot (v2.10.0) (Street et al., 2018). The code of the data analysis has been
884 made available at GitHub (https://github.com/devneurolab/scRNAseq_Hglaberrima).
885

886 ## *HCR-FISH*

887
888 Regenerating intestines from animals eviscerated 8-9 days previously and intestines from non-eviscerated (controls)
889 animals were collected and fixed in 4% (v/v) paraformaldehyde with phosphate-buffered saline (0.01M PBS; 0.138M
890 NaCl; 0.0027M KCl; pH7.4) overnight at 4 °C. Tissues were then, washed three times by PBS, and treated overnight
891 with 40% saccharose prior to cutting in the cryostat. Sections (20 mm) were prepared in a cryostat (Leica CM1850),
892 as previously published for immunohistochemistry (Reyes-Rivera et al., 2024). Gene spatial expression was
893 determined by designing twelve (12) or twenty (24) set split probes for each gene marker. To decrease probe

894 unspecific binding and increase its signal to background ratio, probes were designed as described by H. Choi and
895 colleagues (Molecular Instruments) (Choi et al., 2018). To ensure probe gene target specificity, all nucleotide
896 regions selected for probe design underwent extensive validation using the newly developed *H. glaberrima* genome
897 and transcriptome alignment tool (https://blastkit.hpcf.upr.edu/hglaberrima-v1/) (Medina-Feliciano et al., 2021).
898 Probes were used at a final concentration of approximately 20-25 nM.
899
900 Immediately after slide preparation, HCR-FISH v3 was carried out using a modified version of Molecular
901 Instrument's fresh fixed frozen tissues protocol. Probe hybridization was conducted overnight at 37 °C, while DNA
902 hairpin amplification (B1-546nm or B2-546nm) was done at 25°C overnight with 3pmol of h1 and h2, respectively.
903 Our protocol modification involved replacing Ethanol with Methanol during sample permeabilization. Also, the use of
904 proteinase K was omitted, and Tween 20 at 0.1% was added to all PBS wash buffers. Once slides were prepared,
905 image acquisition was attained using a Nikon DS-Qi2 fluorescent microscope. Positive control probes (PolyA) were
906 used as signal calibrators to define background from positive signal during image analysis.
907

908 ## Acknowledgements

909
910 We thank the funding support from the National Institute of Health (NIH) under the grant number 2R15GM124595.
911 Also funding support was provided by the NIH Research Initiative for Scientific Enhancement (RISE) program to
912 Y.M.N under grant number 5R25GM061151-22. We acknowledge the High-Performance Computing Facility of the
913 University of Puerto Rico sponsored by the University of Puerto Rico and the Institutional Development Award
914 (IDeA) INBRE grant P20 GM103475 from the National Institute for General Medical Sciences (NIGMS), a
915 component of the NIH and the Bioinformatics Research Core of INBRE. We would also like to acknowledge our
916 colleague Joseph F. Ryan for his constructive feedback and computational resources.
917

918 ## Data Availability

919 Data generated during this project has been made publicly available at Figshare (Medina-Feliciano et al.,
920 2024) including raw and processed sequencing data.
921
922
923
924

References

Alicea-Delgado M, García-Arrarás JE. 2021. Wnt/β-catenin signaling pathway regulates cell proliferation but not muscle dedifferentiation nor apoptosis during sea cucumber intestinal regeneration. *Dev Biol* **480**:105–113. doi:10.1016/j.ydbio.2021.08.011

Alvarado AS, Tsonis PA. 2006. Bridging the regeneration gap: Genetic insights from diverse animal models. *Nat Rev Genet*. doi:10.1038/nrg1923

Anderson D, Skut P, Hughes AM, Ferrari E, Tickner J, Xu J, Mullin BH, Tang D, Malinge S, Kees UR, Kotecha RS, Lassmann T, Cheung LC. 2020. The bone marrow microenvironment of pre-B acute lymphoblastic leukemia at single-cell resolution. *Sci Rep* **10**. doi:10.1038/s41598-020-76157-4

Auger NA, Medina-Feliciano JG, Quispe-Parra DJ, Colón-Marrero S, Ortiz-Zuazaga H, García-Arrarás JE. 2023. Characterization and Expression of Holothurian Wnt Signaling Genes during Adult Intestinal Organogenesis. *Genes (Basel)* **14**. doi:10.3390/genes14020309

Ayyaz A, Kumar S, Sangiorgi B, Ghoshal B, Gosio J, Ouladan S, Fink M, Barutcu S, Trcka D, Shen J, Chan K, Wrana JL, Gregorieff A. 2019. Single-cell transcriptomes of the regenerating intestine reveal a revival stem cell. *Nature* **569**:121–125. doi:10.1038/s41586-019-1154-y

Aztekin C. 2021. Tissues and Cell Types of Appendage Regeneration: A Detailed Look at the Wound Epidermis and Its Specialized Forms. *Front Physiol* **12**. doi:10.3389/fphys.2021.771040

Baguñà J. 2012. The planarian neoblast: The rambling history of its origin and some current black boxes. *International Journal of Developmental Biology* **56**. doi:10.1387/ijdb.113463jb

Barela Hudgell MA, Grayfer L, Smith LC. 2022. Coelomocyte populations in the sea urchin, Strongylocentrotus purpuratus, undergo dynamic changes in response to immune challenge. *Front Immunol* **13**. doi:10.3389/fimmu.2022.940852

Bello SA, Abreu-Irizarry RJ, García-Arrarás JE. 2015. Primary cell cultures of regenerating holothurian tissues. *Methods in Molecular Biology* **1189**:283–297. doi:10.1007/978-1-4939-1164-6_19

Bello SA, Torres-Gutiérrez V, Rodríguez-Flores EJ, Toledo-Román EJ, Rodríguez N, Díaz-Díaz LM, Vázquez-Figueroa LD, Cuesta JM, Grillo-Alvarado V, Amador A, Reyes J, García-Arrarás JE. 2020. Insights into intestinal regeneration signaling mechanisms. *Dev Biol* **458**:12–31. doi:10.1016/j.ydbio.2019.10.005

Beumer J, Clevers H. 2021. Cell fate specification and differentiation in the adult mammalian intestine. *Nat Rev Mol Cell Biol*. doi:10.1038/s41580-020-0278-0

Bhattacharjee A, Pal S, Feldman GM, Cathcart MK. 2011. Hck is a key regulator of gene expression in alternatively activated human monocytes. *Journal of Biological Chemistry* **286**:36709–36723. doi:10.1074/jbc.M111.291492

Bokel C, Brown NH. 2002. Review Integrins in Development: Moving on, Responding to, and Sticking to the Extracellular Matrix. *Dev Cell* **3**:311–321.

Bradford DK, Cole SJ, Cooper HM. 2009. Netrin-1: Diversity in development. *International Journal of Biochemistry and Cell Biology*. doi:10.1016/j.biocel.2008.03.014

Busslinger GA, Weusten BLA, Bogte A, Begthel H, Brosens LAA, Clevers H. 2021. Human gastrointestinal epithelia of the esophagus, stomach, and duodenum resolved at single-cell resolution. *Cell Rep* **34**. doi:10.1016/j.celrep.2021.108819

Byrne M. 2023. Autotomy, evisceration, and regeneration in dendrochirotid holothuroidsThe World of Sea Cucumbers: Challenges, Advances, and Innovations. doi:10.1016/B978-0-323-95377-1.00034-5

Byrne M, Koop D, Strbenac D, Cisternas P, Balogh R, Yang JYH, Davidson PL, Wray G. 2020. Transcriptomic analysis of sea star development through metamorphosis to the highly derived pentameral body plan with a focus on neural transcription factors. *DNA Research* **27**. doi:10.1093/dnares/dsaa007

Cabrera-Serrano A, García-Arrarás JE. 2004. RGD-containing peptides inhibit intestinal regeneration in the sea cucumber Holothuria glaberrimaDevelopmental Dynamics. pp. 171–178. doi:10.1002/dvdy.20112

Candelaria AG, Murray G, File SK, García-Arrarás JE. 2006. Contribution of mesenterial muscle dedifferentiation to intestine regeneration in the sea cucumber Holothuria glaberrima. *Cell Tissue Res* **325**:55–65. doi:10.1007/s00441-006-0170-z

Candia-Carnevali MD, Sugni M, Bonasoro F. 2024. Regeneration Potential in Echinoderms: Revisiting the Regeneration ConceptFrontiers in Invertebrate Physiology: A Collection of Reviews: Volume 3: Annelida and Echinodermata. doi:10.1201/9781003405184-5

979 Candia-Carnevali MD, Thorndyke MC, Matranga V. 2009. Regenerating echinoderms: A promise to
980 understand stem cells potentialStem Cells in Marine Organisms. Springer Netherlands. pp. 165–186.
981 doi:10.1007/978-90-481-2767-2_7
982 Capdevila C, Trifas M, Miller J, Anderson T, Sims PA, Yan KS. 2021. Cellular origins and lineage
983 relationships of the intestinal epithelium. *Am J Physiol Gastrointest Liver Physiol*.
984 doi:10.1152/ajpgi.00188.2021
985 Carlson BM. 2007. Principles of Regenerative Biology, Principles of Regenerative Biology. doi:10.1016/B978-
986 0-12-369439-3.X5000-4
987 Chen M, Menon MC, Wang W, Fu J, Yi Z, Sun Z, Liu J, Li Z, Mou L, Banu K, Lee SW, Dai Y, Anandakrishnan
988 N, Azeloglu EU, Lee K, Zhang W, Das B, He JC, Wei C. 2023. HCK induces macrophage activation to
989 promote renal inflammation and fibrosis via suppression of autophagy. *Nat Commun* **14**.
990 doi:10.1038/s41467-023-40086-3
991 Choi HMT, Schwarzkopf M, Fornace ME, Acharya A, Artavanis G, Stegmaier J, Cunha A, Pierce NA. 2018.
992 Third-generation in situ hybridization chain reaction: Multiplexed, quantitative, sensitive, versatile,
993 robust. *Development (Cambridge)* **145**. doi:10.1242/dev.165753
994 Cocurullo M, Paganos P, Annunziata R, Voronov D, Arnone MI. 2023. Single-Cell Transcriptomic Analysis
995 Reveals the Molecular Profile of Go-Opsin Photoreceptor Cells in Sea Urchin Larvae. *Cells* **12**.
996 doi:10.3390/cells12172134
997 Courtney Smith L, Arizza V, Barela Hudgell MA, Barone G, Bodnar AG, Buckley KM, Cunsolo V, Dheilly NM,
998 Franchi N, Fugmann SD, Furukawa R, Garcia-Arraras J, Henson JH, Hibino T, Irons ZH, Li C, Lun CM,
999 Majeske AJ, Oren M, Pagliara P, Pinsino A, Raftos DA, Rast JP, Samasa B, Schillaci D, Schrankel CS,
1000 Stabili L, Stensväg K, Sutton E. 2018. Echinodermata: The complex immune system in
1001 echinodermsAdvances in Comparative Immunology. Springer International Publishing. pp. 409–501.
1002 doi:10.1007/978-3-319-76768-0_13
1003 Cox MK, Appelboom BL, Ban GI, Serra R. 2014. Erg cooperates with TGF-β to control mesenchymal
1004 differentiation. *Exp Cell Res* **328**:410–418. doi:10.1016/j.yexcr.2014.08.015
1005 Dewing JM, Carare RO, Lotery AJ, Ratnayaka JA. 2020. The diverse roles of TIMP-3: Insights into
1006 degenerative diseases of the senescent retina and brain. *Cells*. doi:10.3390/cells9010039
1007 Dhordain P, Dewittea F, Desbiensb X, Stehelin D, Duterque-Coquillaud M. 1995. Mesodermal expression of
1008 the chicken erg gene associated with precartilaginous condensation and cartilage differentiation,
1009 Mechanisms of Development.
1010 Diaz-Balzac CA, Santacana-Laffitte G, San Miguel-Ruiz JE, Tossas K, Valentin-Tirado G, Rives-Sanchez M,
1011 Mesleh A, Torres II, Garcia-Arraras JE. 2007. Identification of Nerve Plexi in Connective Tissues of the
1012 Sea Cucumber Holothuria glaberrima by Using a Novel Nerve-Specific Antibody.
1013 Diaz-Miranda L, Blanco RE, Garcia-Arraras JE. 1995. Localization of the Heptapeptide GFSKLYFamide in
1014 the Sea Cucumber Holothuria glaberrima (Echinodermata): A Light and Electron Microscopic Study. *J*
1015 *Comp Neurol* **352**:626–640.
1016 Dolgachev V, Panicker S, Balijepalli S, McCandless LK, Yin Y, Swamy S, Suresh M V., Delano MJ, Hemmila
1017 MR, Raghavendran K, Machado-Aranda D. 2018. Electroporation-mediated delivery of FER gene
1018 enhances innate immune response and improves survival in a murine model of pneumonia. *Gene Ther*
1019 **25**:359–375. doi:10.1038/s41434-018-0022-y
1020 Dolmatov IY. 2021. Molecular aspects of regeneration mechanisms in holothurians. *Genes (Basel)*.
1021 doi:10.3390/genes12020250
1022 Dolmatov IY, Nizhnichenko VA. 2023. Extracellular Matrix of Echinoderms. *Mar Drugs*.
1023 doi:10.3390/md21070417
1024 Dong C, Muriel JM, Ramirez S, Hutter H, Hedgecock EM, Breydo L, Baskakov I V., Vogel BE. 2006.
1025 Hemicentin assembly in the extracellular matrix is mediated by distinct structural modules. *Journal of*
1026 *Biological Chemistry* **281**:23606–23610. doi:10.1074/jbc.M513589200
1027 Dumitru CA, Bankfalvi A, Gu X, Zeidler R, Brandau S, Lang S. 2013. AHNAK and Inflammatory Markers
1028 Predict Poor Survival in Laryngeal Carcinoma. *PLoS One* **8**. doi:10.1371/journal.pone.0056420
1029 Dunn LL, Sekyer EO, Suryo Rahmanto Y, Richardson DR. 2006. The function of melanotransferrin: A role in
1030 melanoma cell proliferation and tumorigenesis. *Carcinogenesis* **27**:2157–2169.
1031 doi:10.1093/carcin/bgl045
1032 Elmentaite R, Ross ADB, Roberts K, James KR, Ortmann D, Gomes T, Nayak K, Tuck L, Pritchard S,
1033 Bayraktar OA, Heuschkel R, Vallier L, Teichmann SA, Zilbauer M. 2020. Single-Cell Sequencing of

Developing Human Gut Reveals Transcriptional Links to Childhood Crohn's Disease. *Dev Cell* **55**:771-783.e5. doi:10.1016/j.devcel.2020.11.010

Foster S, Oulhen N, Fresques T, Zaki H, Wessel G. 2022. Single-cell RNA-sequencing analysis of early sea star development. *Development (Cambridge)* **149**. doi:10.1242/dev.200982

García-Arrarás JE, Bello SA, Malavez S. 2019. The mesentery as the epicenter for intestinal regeneration. *Semin Cell Dev Biol*. doi:10.1016/j.semcdb.2018.09.001

García-Arrarás JE, Estrada-Rodgers L, Santiago R, Torres II, Díaz-Miranda L, Torres-Avillán I. 1998. Cellular mechanisms of intestine regeneration in the sea cucumber, Holothuria glaberrima selenka (Holothuroidea:Echinodermata). *Journal of Experimental Zoology* **281**:288–304. doi:10.1002/(SICI)1097-010X(19980701)281:4<288::AID-JEZ5>3.0.CO;2-K

García-Arrarás JE, Schenk C, Rodrígues-Ramírez R, Torres II, Valentín G, Candelaria AG. 2006. Spherulocytes in the echinoderm Holothuria glaberrima and their involvement in intestinal regeneration. *Developmental Dynamics* **235**:3259–3267. doi:10.1002/dvdy.20983

García-Arrarás JE, Valentín-Tirado G, Flores JE, Rosa RJ, Rivera-Cruz A, San Miguel-Ruiz JE, Tossas K. 2011. Cell dedifferentiation and epithelial to mesenchymal transitions during intestinal regeneration in H. glaberrima. *BMC Dev Biol* **11**. doi:10.1186/1471-213X-11-61

Gemberling M, Bailey TJ, Hyde DR, Poss KD. 2013. The zebrafish as a model for complex tissue regeneration. *Trends in Genetics*. doi:10.1016/j.tig.2013.07.003

Gerber T, Murawala P, Knapp D, Masselink W, Schuez M, Hermann S, Gac-Santel M, Nowoshilow S, Kageyama J, Khattak S, Currie JD, Camp JG, Tanaka EM, Treutlein B. 2018. Single-cell analysis uncovers convergence of cell identities during axolotl limb regeneration. *Science (1979)* **362**. doi:10.1126/science.aaq0681

Globus M, Vethamany-Globus S, Lee YCI. 1980. Effect of apical epidermal cap on mitotic cycle and cartilage differentiation in regeneration blastemata in the newt, Notophthalmus viridescens. *Dev Biol* **75**. doi:10.1016/0012-1606(80)90169-4

Gluck C, Glathar A, Tsompana M, Nowak N, Garrett-Sinha LA, Buck MJ, Sinha S. 2019. Molecular dissection of the oncogenic role of ETS1 in the mesenchymal subtypes of head and neck squamous cell carcinoma. *PLoS Genet* **15**. doi:10.1371/journal.pgen.1008250

Grabski IN, Street K, Irizarry RA. 2023. Significance analysis for clustering with single-cell RNA-sequencing data. *Nat Methods* **20**. doi:10.1038/s41592-023-01933-9

Guatelli S, Ferrario C, Bonasoro F, Anjo SI, Manadas B, Candia Carnevali MD, Varela Coelho A, Sugni M. 2022. More than a simple epithelial layer: multifunctional role of echinoderm coelomic epithelium. *Cell Tissue Res* **390**:207–227. doi:10.1007/s00441-022-03678-x

Hanington PC, Zhang SM. 2011. The primary role of fibrinogen-related proteins in invertebrates is defense, not coagulation. *J Innate Immun* **3**:17–27. doi:10.1159/000321882

Hao Y, Hao S, Andersen-Nissen E, Mauck WM, Zheng S, Butler A, Lee MJ, Wilk AJ, Darby C, Zager M, Hoffman P, Stoeckius M, Papalexi E, Mimitou EP, Jain J, Srivastava A, Stuart T, Fleming LM, Yeung B, Rogers AJ, McElrath JM, Blish CA, Gottardo R, Smibert P, Satija R. 2021. Integrated analysis of multimodal single-cell data. *Cell* **184**:3573-3587.e29. doi:10.1016/j.cell.2021.04.048

Hao Y, Stuart T, Kowalski MH, Choudhary S, Hoffman P, Hartman A, Srivastava A, Molla G, Madad S, Fernandez-Granda C, Satija R. 2024. Dictionary learning for integrative, multimodal and scalable single-cell analysis. *Nat Biotechnol* **42**:293–304. doi:10.1038/s41587-023-01767-y

Hetzel HR. 1963. Studies on Holothurian Coelomocytes. I. A Survey of Coelomocyte Types, Bulletin.

Huang Y, Laval SH, Remoortere A, Baudier J, Benaud C, Anderson LVB, Straub V, Deelder A, Frants RR, Dunnen JT, Bushby K, Maarel SM. 2007. AHNAK a novel component of the dysferlin protein complex, redistributes to the cytoplasm with dysferlin during skeletal muscle regeneration. *The FASEB Journal* **21**:732–742. doi:10.1096/fj.06-6628com

Humbert PO, Verona R, Trimarchi JM, Rogers C, Dandapani S, Lees JA. 2000. E2f3 is critical for normal cellular proliferation.

Iwamoto M, Higuchi Y, Enomoto-Iwamoto M, Kurisu K, Koyama E, Yeh H, Rosenbloom J, Pacifici M. 2001. The role of ERG (ets related gene) in cartilage development. *Osteoarthritis Cartilage* **9**. doi:10.1053/joca.2001.0443

Juliano CE, Reich A, Liu N, Götzfried J, Zhong M, Uman S, Reenan RA, Wessel GM, Steele RE, Lin H. 2014. PIWI proteins and PIWI-interacting RNAs function in Hydra somatic stem cells. *Proc Natl Acad Sci U S A* **111**:337–342. doi:10.1073/pnas.1320965111

King HO, Owusu-Boaitey KE, Fincher CT, Reddien PW. 2024. A transcription factor atlas of stem cell fate in planarians. *Cell Rep* **43**. doi:10.1016/j.celrep.2024.113843

Koga H, Matsubara M, Fujitani H, Miyamoto N, Komatsu M, Kiyomoto M, Akasaka K, Wada H. 2010. Functional evolution of Ets in echinoderms with focus on the evolution of echinoderm larval skeletons. *Dev Genes Evol* **220**:107–115. doi:10.1007/s00427-010-0333-5

La Manno G, Soldatov R, Zeisel A, Braun E, Hochgerner H, Petukhov V, Lidschreiber K, Kastriti ME, Lönnerberg P, Furlan A, Fan J, Borm LE, Liu Z, van Bruggen D, Guo J, He X, Barker R, Sundström E, Castelo-Branco G, Cramer P, Adameyko I, Linnarsson S, Kharchenko P V. 2018. RNA velocity of single cells. *Nature* **560**:494–498. doi:10.1038/s41586-018-0414-6

Leigh ND, Dunlap GS, Johnson K, Mariano R, Oshiro R, Wong AY, Bryant DM, Miller BM, Ratner A, Chen A, Ye WW, Haas BJ, Whited JL. 2018. Transcriptomic landscape of the blastema niche in regenerating adult axolotl limbs at single-cell resolution. *Nat Commun* **9**. doi:10.1038/s41467-018-07604-0

Lin TY, Gerber T, Taniguchi-Sugiura Y, Murawala P, Hermann S, Grosser L, Shibata E, Treutlein B, Tanaka EM. 2021. Fibroblast dedifferentiation as a determinant of successful regeneration. *Dev Cell* **56**:1541-1551.e6. doi:10.1016/j.devcel.2021.04.016

Lindsay-Mosher N, Chan A, Pearson BJ. 2020. Planarian EGF repeat-containing genes megf6 and hemicentin are required to restrict the stem cell compartment. *PLoS Genet* **16**. doi:10.1371/journal.pgen.1008613

Locard-Paulet M, Palasca O, Jensen LJ. 2022. Identifying the genes impacted by cell proliferation in proteomics and transcriptomics studies. *PLoS Comput Biol* **18**. doi:10.1371/journal.pcbi.1010604

Lõoke M, Maloney MF, Bell SP. 2017. Mcm10 regulates DNA replication elongation by stimulating the CMG replicative helicase. doi:10.1101/gad.291336

Lu H, Shi X, Wu G, Zhu J, Song C, Zhang Q, Yang G. 2015. FGF13 regulates proliferation and differentiation of skeletal muscle by down-regulating Spry1. *Cell Prolif* **48**:550–560. doi:10.1111/cpr.12200

Magnussen SN, Toraskar J, Hadler-olsen E, Steigedal TS, Svineng G. 2021. Nephronectin as a matrix effector in cancer. *Cancers (Basel)*. doi:10.3390/cancers13050959

Makanae A, Mitogawa K, Satoh A. 2014. Co-operative Bmp- and Fgf-signaling inputs convert skin wound healing to limb formation in urodele amphibians. *Dev Biol* **396**:57–66. doi:10.1016/j.ydbio.2014.09.021

Mantri M, Scuderi GJ, Abedini-Nassab R, Wang MFZ, McKellar D, Shi H, Grodner B, Butcher JT, De Vlaminck I. 2021. Spatiotemporal single-cell RNA sequencing of developing chicken hearts identifies interplay between cellular differentiation and morphogenesis. *Nat Commun* **12**. doi:10.1038/s41467-021-21892-z

Mashanov V, Zueva O, Mashanova D, García-Arrarás JE. 2017. Expression of stem cell factors in the adult sea cucumber digestive tube. *Cell Tissue Res* **370**:427–440. doi:10.1007/s00441-017-2692-y

Mashanov VS, Dolmatov IY, Heinzeller T, Mashanov VS, Dolmatov IY, Heinzeller T. 2005. Transdifferentiation in Holothurian Gut Regeneration. *Biological Bulletin Marine Biological Laboratory* **209**:184–193.

Mashanov VS, Zueva O, García-Arrarás JE. 2014. Postembryonic Organogenesis of the Digestive Tube: Why Does It Occur in Worms and Sea Cucumbers but Fail in Humans?Current Topics in Developmental Biology. doi:10.1016/B978-0-12-391498-9.00006-1

Mashanov VS, Zueva OR, García-Arrarás JE. 2015. Expression of pluripotency factors in echinoderm regeneration. *Cell Tissue Res* **359**:521–536. doi:10.1007/s00441-014-2040-4

Mashanov VS, Zueva OR, Garcia-Arraras JE. 2012. Expression of Wnt9, TCTP, and Bmp1/Tll in sea cucumber visceral regeneration. *Gene Expression Patterns* **12**:24–35. doi:10.1016/j.gep.2011.10.003

Mashanov VS, Zueva OR, Rojas-Catagena C, Garcia-Arraras JE. 2010. Visceral regeneration in a sea cucumber involves extensive expression of survivin and mortalin homologs in the mesothelium. *BMC Dev Biol* **10**. doi:10.1186/1471-213X-10-117

Medina-Feliciano JG, García-Arrarás JE. 2021. Regeneration in Echinoderms: Molecular Advancements. *Front Cell Dev Biol*. doi:10.3389/fcell.2021.768641

Medina-Feliciano JG, Pirro S, García-Arrarás JE, Mashanov V, Ryan JF. 2021. Draft Genome of the Sea Cucumber Holothuria glaberrima, a Model for the Study of Regeneration. *Front Mar Sci* **8**. doi:10.3389/fmars.2021.603410

Medina-Feliciano JG, Valentín-Tirado G, Luna-Martinez K, Miranda-Negron Y, Garcia-Arraras JE. 2024. Single-cell RNA sequencing of the holothurian regenerating intestine. doi:https://doi.org/10.6084/m9.figshare.c.7289770

Meyer A, Ku C, Hatleberg WL, Telmer CA, Hinman V. 2023. New hypotheses of cell type diversity and novelty from orthology-driven comparative single cell and nuclei transcriptomics in echinoderms. *Elife* **12**. doi:10.7554/eLife.80090

Min S, Whited JL. 2023. Limb blastema formation: How much do we know at a genetic and epigenetic level? *Journal of Biological Chemistry*. doi:10.1016/j.jbc.2022.102858

Mishra L, Derynck R, Mishra B. 2005. Transforming Growth Factor-b Signaling in Stem Cells and Cancer Roles of TGF-b Family Members in Neural Stem Cells. *Science (1979)*.

Mochmann LH, Neumann M, Von Der Heide EK, Nowak V, Kühl AA, Ortiz-Tanchez J, Bock J, Hofmann WK, Baldus CD. 2013. ERG induces a mesenchymal-like state associated with chemoresistance in leukemia cells. *Oncotarget* **5**.

Murray G, García-Arrarás JE. 2004. Myogenesis during holothurian intestinal regeneration. *Cell Tissue Res* **318**:515–524. doi:10.1007/s00441-004-0978-3

Nieves-Ríos C, Alvarez-Falcón S, Malavez S, Rodriguez-Otero J, García-Arrarás JE. 2020. The nervous system component of the mesentery of the sea cucumber Holothuria glaberrima in normal and regenerating animals. *Cell Tissue Res* **380**:67–77. doi:10.1007/s00441-019-03142-3

Nishimoto S, Nishida E. 2007. Fibroblast growth factor 13 is essential for neural differentiation in Xenopus early embryonic development. *Journal of Biological Chemistry* **282**:24255–24261. doi:10.1074/jbc.M704277200

Oike Y, Yasunaga K, Suda T. 2004. Angiopoietin-related/angiopoietin-like proteins regulate angiogenesis. *Int J Hematol*. doi:10.1532/IJH97.04034

Ortiz-Pineda PA, Ramírez-Gómez F, Pérez-Ortiz J, González-Díaz S, Santiago-De Jesús F, Hernández-Pasos J, Del Valle-Avila C, Rojas-Cartagena C, Suárez-Castillo EC, Tossas K, Méndez-Merced AT, Roig-López JL, Ortiz-Zuazaga H, García-Arrarás JE. 2009. Gene expression profiling of intestinal regeneration in the sea cucumber. *BMC Genomics* **10**. doi:10.1186/1471-2164-10-262

Paganos P, Ronchi P, Carl J, Mizzon G, Martinez P, Benvenuto G, Arnone MI. 2022a. Integrating single cell transcriptomics and volume electron microscopy confirms the presence of pancreatic acinar-like cells in sea urchins. *Front Cell Dev Biol* **10**. doi:10.3389/fcell.2022.991664

Paganos P, Ullrich-Lüter E, Caccavale F, Zakrzewski A, Voronov D, Fournon-Berodia I, Cocurullo M, Lüter C, Arnone MI. 2022b. A New Model Organism to Investigate Extraocular Photoreception: Opsin and Retinal Gene Expression in the Sea Urchin Paracentrotus lividus. *Cells* **11**. doi:10.3390/cells11172636

Paganos P, Voronov D, Musser JM, Arendt D, Arnone MI. 2021. Single-cell RNA sequencing of the Strongylocentrotus purpuratus larva reveals the blueprint of major cell types and nervous system of a non-chordate deuterostome. *Elife* 1–29. doi:https://doi.org/10.7554/eLife.70416

Pagès H, Carlson M, Falcon S, Li N. 2024. AnnotationDbi: Manipulation of SQLite-based annotations in Bioconductor. . doi:10.18129/B9.bioc.AnnotationDbi

Parigi SM, Larsson L, Das S, Ramirez Flores RO, Frede A, Tripathi KP, Diaz OE, Selin K, Morales RA, Luo X, Monasterio G, Engblom C, Gagliani N, Saez-Rodriguez J, Lundeberg J, Villablanca EJ. 2022. The spatial transcriptomic landscape of the healing mouse intestine following damage. *Nat Commun* **13**. doi:10.1038/s41467-022-28497-0

Piovani L, Czarkwiani A, Ferrario C, Sugni M, Oliveri P. 2021. Ultrastructural and molecular analysis of the origin and differentiation of cells mediating brittle star skeletal regeneration. *BMC Biol* **19**. doi:10.1186/s12915-020-00937-7

Poh AR, O'donoghue RJJ, Ernst M. 2015. Hematopoietic cell kinase (HCK) as a therapeutic target in immune and cancer cells.

Poleo G, Brown CW, Laforest L, Akimenko MA. 2001. Cell proliferation and movement during early fin regeneration in zebrafish. *Developmental Dynamics*. doi:10.1002/dvdy.1152

Quiñones JL, Rosa R, Ruiz DL, García-Arrarás JE. 2002. Extracellular matrix remodeling and metalloproteinase involvement during intestine regeneration in the sea cucumber Holothuria glaberrima. *Dev Biol* **250**:181–197. doi:10.1006/dbio.2002.0778

Quispe-Parra D, Valentín G, García-Arrarás JE. 2021. A roadmap for intestinal regeneration. *International Journal of Developmental Biology* **65**:427–437. doi:10.1387/ijdb.200227dq

Quispe-Parra DJ, Medina-Feliciano JG, Cruz-González S, Ortiz-Zuazaga H, García-Arrarás JE. 2021. Transcriptomic analysis of early stages of intestinal regeneration in Holothuria glaberrima. *Sci Rep* **11**. doi:10.1038/s41598-020-79436-2

Ramírez-Gómez F, Aponte-Rivera F, Méndez-Castaner L, García-Arrarás JE. 2010. Changes in holothurian coelomocyte populations following immune stimulation with different molecular patterns. *Fish Shellfish Immunol* **29**:175–185. doi:10.1016/j.fsi.2010.03.013

Reddien PW. 2018. The Cellular and Molecular Basis for Planarian Regeneration. *Cell*. doi:10.1016/j.cell.2018.09.021

Reyes-Rivera J, Grillo-Alvarado V, Soriano-López AE, García-Arrarás JE. 2024. Evidence of interactions among apoptosis, cell proliferation, and dedifferentiation in the rudiment during whole-organ intestinal regeneration in the sea cucumber. *Dev Biol* **505**. doi:10.1016/j.ydbio.2023.11.001

Rizzo F, Fernandez-Serra M, Squarzoni P, Archimandritis A, Arnone MI. 2006. Identification and developmental expression of the ets gene family in the sea urchin (Strongylocentrotus purpuratus). *Dev Biol* **300**:35–48. doi:10.1016/j.ydbio.2006.08.012

Rodgers AK, Smith JJ, Voss SR. 2020. Identification of immune and non-immune cells in regenerating axolotl limbs by single-cell sequencing. *Exp Cell Res*. doi:10.1016/j.yexcr.2020.112149

Rojas-Cartagena C, Ortíz-Pineda P, Ramírez-Gómez F, Suárez-Castillo EC, Matos-Cruz V, Rodríguez C, Ortíz-Zuazaga H, García-Arrarás JE. 2007. Distinct profiles of expressed sequence tags during intestinal regeneration in the sea cucumber Holothuria glaberrima. *Physiol Genomics* **31**:203–215. doi:10.1152/physiolgenomics.00228.2006.-Repair

Rosado-Olivieri EA, Ramos-Ortiz GA, Hernández-Pasos J, Díaz-Balzac CA, Vázquez-Rosa E, Valentín-Tirado G, Vega IE, García-Arrarás JE, Biochem Physiol Biochem Mol Biol Author manuscript CB. 2017. A START-Domain-containing Protein is a Novel Marker of Nervous System Components of the Sea Cucumber Holothuria glaberrima HHS Public Access Author manuscript. *Comp Biochem Physiol B Biochem Mol Biol* **214**:57–65. doi:10.1016/j.cbpb

Roy S, Gatien S. 2008. Regeneration in axolotls: a model to aim for! *Exp Gerontol*. doi:10.1016/j.exger.2008.09.003

Santiago P, Roig-López L, Santiago C, García-Arrarás JE. 2000. Serum Amyloid A Protein in an Echinoderm: Its Primary Structure and Expression During Intestinal Regeneration in the Sea Cucumber Holothuria glaberrima, JOURNAL OF EXPERIMENTAL ZOOLOGY.

Santos-Ruiz L, Santamaría JA, Ruiz-Sánchez J, Becerra J. 2002. Cell proliferation during blastema formation in the regenerating teleost fin. *Developmental Dynamics* **223**:262–272. doi:10.1002/dvdy.10055

Satija R, Farrell JA, Gennert D, Schier AF, Regev A. 2015. Spatial reconstruction of single-cell gene expression data. *Nat Biotechnol* **33**:495–502. doi:10.1038/nbt.3192

Satoh N, Hisata K, Foster S, Morita S, Nishitsuji K, Oulhen N, Tominaga H, Wessel GM. 2022. A single-cell RNA-seq analysis of Brachyury-expressing cell clusters suggests a morphogenesis-associated signal center of oral ectoderm in sea urchin embryos. *Dev Biol* **483**:128–142. doi:10.1016/j.ydbio.2022.01.005

Scimone ML, Cloutier JK, Maybrun CL, Reddien PW. 2022. The planarian wound epidermis gene equinox is required for blastema formation in regeneration. *Nat Commun* **13**. doi:10.1038/s41467-022-30412-6

Seifert AW, Muneoka K. 2018. The blastema and epimorphic regeneration in mammals. *Dev Biol*. doi:10.1016/j.ydbio.2017.08.007

Sharlaimova N, Shabelnikov S, Bobkov D, Martynova M, Bystrova O, Petukhova O. 2021. Coelomocyte replenishment in adult Asterias rubens: the possible ways. *Cell Tissue Res* **383**:1043–1060. doi:10.1007/s00441-020-03337-z/Published

Shuttleworth EE. 2018. The role of integrin αvβ8 on human monocytes and macrophages in intestinal immune homeostasis.

Smiley S. 1994. Holothuroidea In: Harrison FW, Chia FS, editors. Microscopic Anatomy of Invertebrates. New York: Wiley-Liss. pp. 401–471.

Smit A, Hubley R. 2015. RepeatModeler Open-1.0.

Smit A, Hubley R, Green P. 2015. RepeatMasker Open-4.0.

Smith LC, Britten RJ, Davidson EH. 1995. Lipopolysaccharide activates the sea urchin immune system, Developmental and Comparative Immunology.

Stamenkovic I. 2003. Extracellular matrix remodelling: The role of matrix metalloproteinases. *Journal of Pathology*. doi:10.1002/path.1400

Stocum DL. 2004. Amphibian Regeneration and Stem Cells. *Curr Top Microbiol Immunol* **280**. doi:https://doi.org/10.1007/978-3-642-18846-6_1

Street K, Risso D, Fletcher RB, Das D, Ngai J, Yosef N, Purdom E, Dudoit S. 2018. Slingshot: Cell lineage and pseudotime inference for single-cell transcriptomics. *BMC Genomics* **19**. doi:10.1186/s12864-018-4772-0

Stuart T, Butler A, Hoffman P, Hafemeister C, Papalexi E, Mauck WM, Hao Y, Stoeckius M, Smibert P, Satija R. 2019. Comprehensive Integration of Single-Cell Data. *Cell* **177**:1888-1902.e21. doi:10.1016/j.cell.2019.05.031

Su F, Yang H, Sun L. 2022. A Review of Histocytological Events and Molecular Mechanisms Involved in Intestine Regeneration in Holothurians. *Biology (Basel)*. doi:10.3390/biology11081095

Sun Y, Kuek V, Qiu H, Tickner J, Chen L, Wang H, He W, Xu J. 2018. The emerging role of NPNT in tissue injury repair and bone homeostasis. *J Cell Physiol*. doi:10.1002/jcp.26013

Tajer B, Savage AM, Whited JL. 2023. The salamander blastema within the broader context of metazoan regeneration. *Front Cell Dev Biol*. doi:10.3389/fcell.2023.1206157

Tanaka EM, Reddien PW. 2011. The Cellular Basis for Animal Regeneration. *Dev Cell*. doi:10.1016/j.devcel.2011.06.016

Telmer CA, Karimi K, Chess MM, Agalakov S, Arshinoff BI, Lotay V, Wang DZ, Chu S, Pells TJ, Vize PD, Hinman VF, Ettensohn CA. 2024. Echinobase: a resource to support the echinoderm research community. *Genetics* **227**. doi:10.1093/genetics/iyae002

Tominaga H, Nishitsuji K, Satoh N. 2023. A single-cell RNA-seq analysis of early larval cell-types of the starfish, Patiria pectinifera: Insights into evolution of the chordate body plan. *Dev Biol* **496**:52–62. doi:10.1016/j.ydbio.2023.01.009

Tossas K, Qi-Huang S, Cuyar E, García-Arrarás JE. 2014. Temporal and spatial analysis of enteric nervous system regeneration in the sea cucumber Holothuria glaberrima . *Regeneration* **1**:10–26. doi:10.1002/reg2.15

Vanden Bossche JP, Jangoux M. 19976. Epithelial origin of starfish coelomocytes. *Nature* **261**:227–228.

Vandenspiegel D, Jangoux M, Flammang P. 2000. Maintaining the Line of Defense: Regeneration of Cuvierian Tubules in the Sea Cucumber Holothuria forskali (Echinodermata, Holothuroidea), Source: Biological Bulletin.

Vázquez-Vélez GE, Rodríguez-Molina JF, Quiñones-Frías MC, García-Arrarás JE. 2016. A proteoglycan-like molecule offers insights into ground substance changes during holothurian intestinal regeneration. *Journal of Histochemistry and Cytochemistry* **64**:381–393. doi:10.1369/0022155416645781

Vlaeminck-Guillem V, Carrere S, Dewitte F, Stehelin D, Desbiens X, Duterque-Coquillaud M. 2000. The Ets family member Erg gene is expressed in mesodermal tissues and neural crests at fundamental steps during mouse embryogenesis. *Mech Dev* 331–335.

Vogg MC, Galliot B, Tsiairis CD. 2019. Model systems for regeneration: Hydra. *Development (Cambridge)* **146**. doi:10.1242/dev.177212

Volkert G, Jahn A, Dinkel C, Fahlbusch F, Zürn C, Hilgers KF, Rascher W, Hartner A, Marek I. 2014. Contribution of the α8 integrin chain to the expression of Extracellular matrix components. *Cell Commun Adhes* **21**:89–98. doi:10.3109/15419061.2013.876012

Wagner DE, Wang IE, Reddien PW. 2011. Clonogenic neoblasts are pluripotent adult stem cells that underlie planarian regeneration. *Science (1979)* **332**. doi:10.1126/science.1203983

Wan J, Zhao X, Liu J, Chen K, Li C. 2022. Src kinase mediates coelomocytes phagocytosis via interacting with focal adhesion kinase in Vibrio splendidus challenged Apostichopus japonicus. *Fish Shellfish Immunol* **124**. doi:10.1016/j.fsi.2022.04.024

Welcker D, Stein C, Feitosa NM, Armistead J, Zhang JL, Lütke S, Kleinridders A, Brüning JC, Eming SA, Sengle G, Niehoff A, Bloch W, Hammerschmidt M. 2021. Hemicentin-1 is an essential extracellular matrix component of the dermal–epidermal and myotendinous junctions. *Sci Rep* **11**. doi:10.1038/s41598-021-96824-4

Xie C, Yao M, Dong Q. 2014. Proliferating cell unclear antigen-associated factor (PAF15): A novel oncogene. *International Journal of Biochemistry and Cell Biology*. doi:10.1016/j.biocel.2014.02.024

Xing K, Yang HS, Chen MY. 2008. Morphological and ultrastructural characterization of the coelomocytes in Apostichopus japonicus. *Aquat Biol* **2**:85–92. doi:10.3354/ab00038

Young MD, Behjati S. 2020. SoupX removes ambient RNA contamination from droplet-based single-cell RNA sequencing data. *Gigascience* **9**. doi:10.1093/gigascience/giaa151

Yu Dolmatov I, Eliseikina Alexander A Bulgakov MG, Ginanova Nina E Lamash Vladimir P Korchagin TT, Dolmatov I, Eliseikina M, Ginanova Lamash TN, Korchagin V, Bulgakov A. 1996. Muscle regeneration in the holothurian Stichopus japonicus, Arch Dev Biol.

Yu G, Wang LG, Han Y, He QY. 2012. ClusterProfiler: An R package for comparing biological themes among gene clusters. *OMICS* **16**:284–287. doi:10.1089/omi.2011.0118

Zeng C, Guo M, Xiang Y, Song M, Xiao K, Li C. 2023. Mesentery AjFGF4–AjFGFR2–ERK pathway modulates intestinal regeneration via targeting cell cycle in echinoderms. *Cell Prolif* **56**. doi:10.1111/cpr.13351

Zenjari C, Boilly-Marer Y, Desbiens X, Oudghir M, Hondermarck H, Benoni Boilly. 1996. Experimental evidence for FGF-' control of blastema cell proliferation during limb regeneration of the Amphibian Pleurodeles waltl 965–971.

Zhao H, Tanegashima K, Ro H, Dawid IB. 2008. Lrig3 regulates neural crest formation in Xenopus by modulating Fgf and Wnt signaling pathways. *Development* **135**:1283–1293. doi:10.1242/dev.015073

Zheng GXY, Terry JM, Belgrader P, Ryvkin P, Bent ZW, Wilson R, Ziraldo SB, Wheeler TD, McDermott GP, Zhu J, Gregory MT, Shuga J, Montesclaros L, Underwood JG, Masquelier DA, Nishimura SY, Schnall-Levin M, Wyatt PW, Hindson CM, Bharadwaj R, Wong A, Ness KD, Beppu LW, Deeg HJ, McFarland C, Loeb KR, Valente WJ, Ericson NG, Stevens EA, Radich JP, Mikkelsen TS, Hindson BJ, Bielas JH. 2017. Massively parallel digital transcriptional profiling of single cells. *Nat Commun* **8**. doi:10.1038/ncomms14049

Supplement

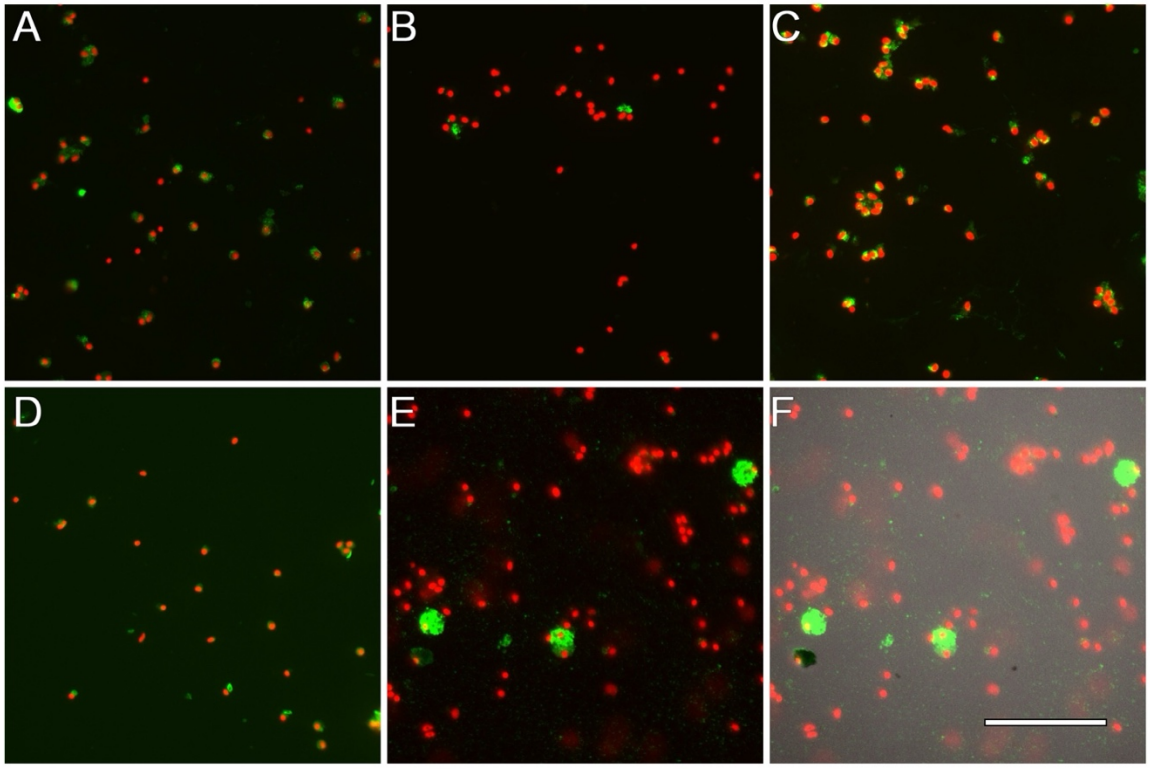

S1 Fig. Labeling of dissociated cell phenotypes with cell markers. Immunocytochemistry, fluorescently labeled phalloidin and Toluidene blue were used to identify various cell populations among the cells dissociated from the mesentery an anlage sample. These include A. a mesenchymal marker (KL4), B. a neuronal marker (RN1), C. a mesothelial marker (Meso1), D. a muscle marker (Phalloidin) and E & F two coelomocyte markers (The antibody SphAA12and toluidine blue). E. Immunocytochemistry using the SphAA12 antibody F. Overlay of toluidene blue labeling (see dark cell on lower left) identifies a different coelomocyte population.

1336
1337
1338
1339

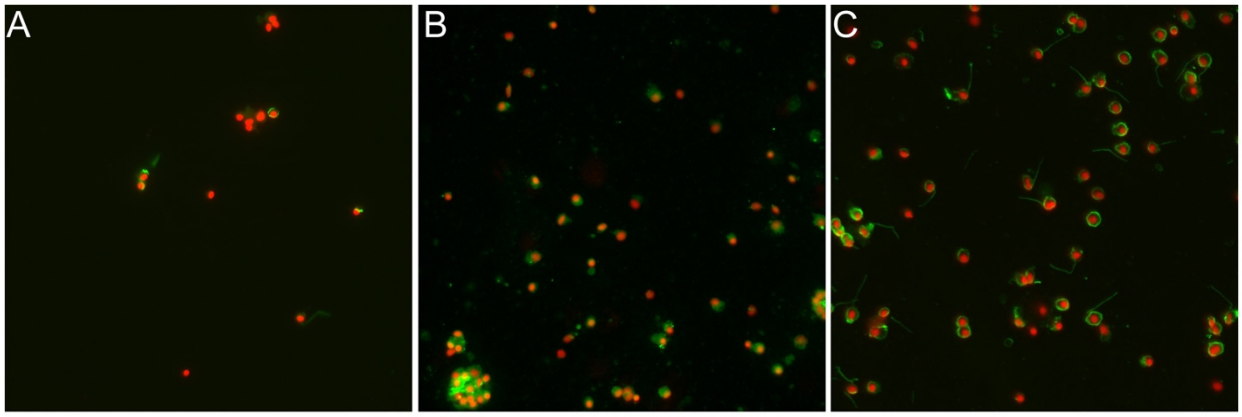

S2 Fig. Immunocytochemical labeling of dissociated cell phenotypes using three different antibodies against tubulin. A. anti-acetylated tubulin labels around 7% of the cells. B. Anti-beta-tubulin labels around 70% of the cells. C. Anti-alpha tubulin labels around 80% of the cells.

1340
1341

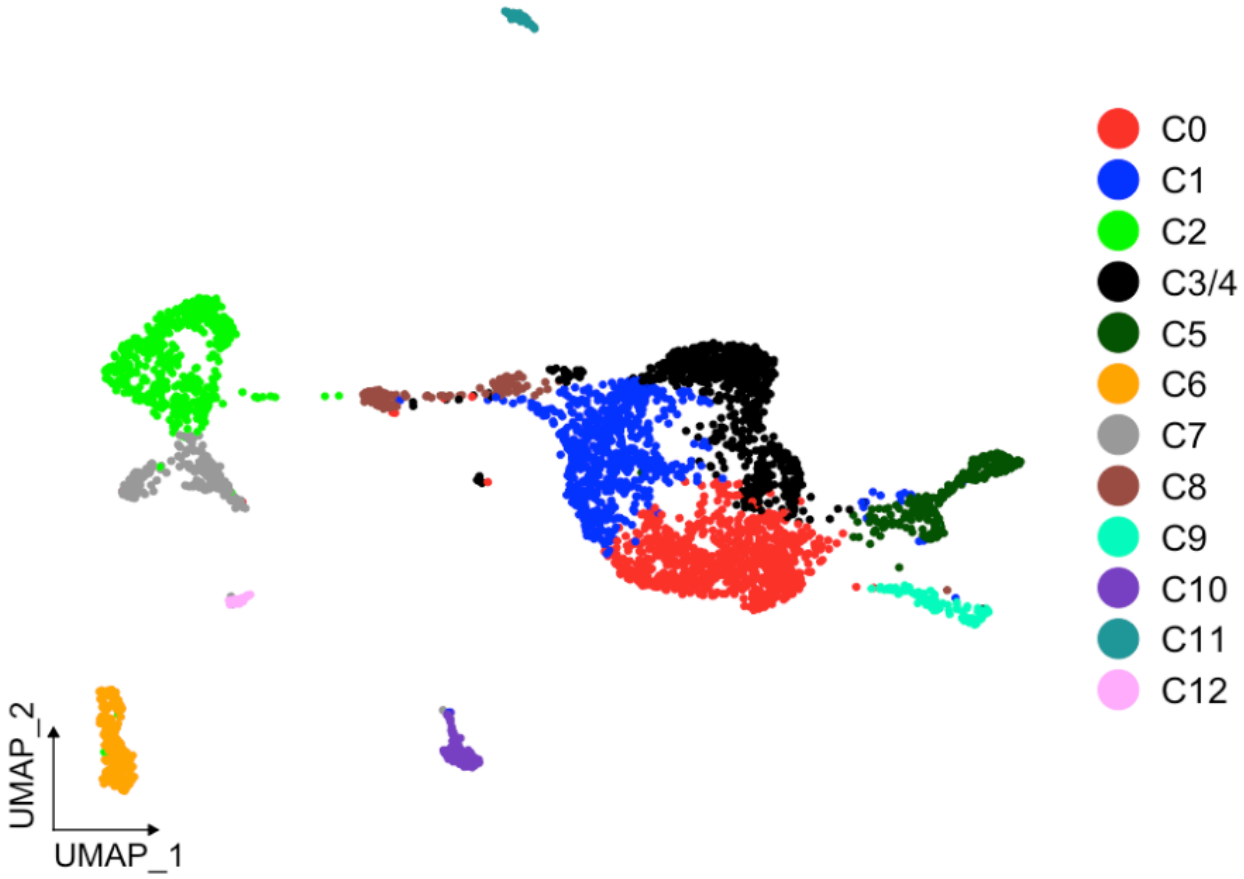

S3 Fig. UMAP of clusters after statistical assessment with scSHC. Results reflect that each of the identified clusters are unique, except for C3 and C4, which it suggests they correspond to a single cluster. All clusters, except for C3/4 (black), are colored as in Fig 1B.

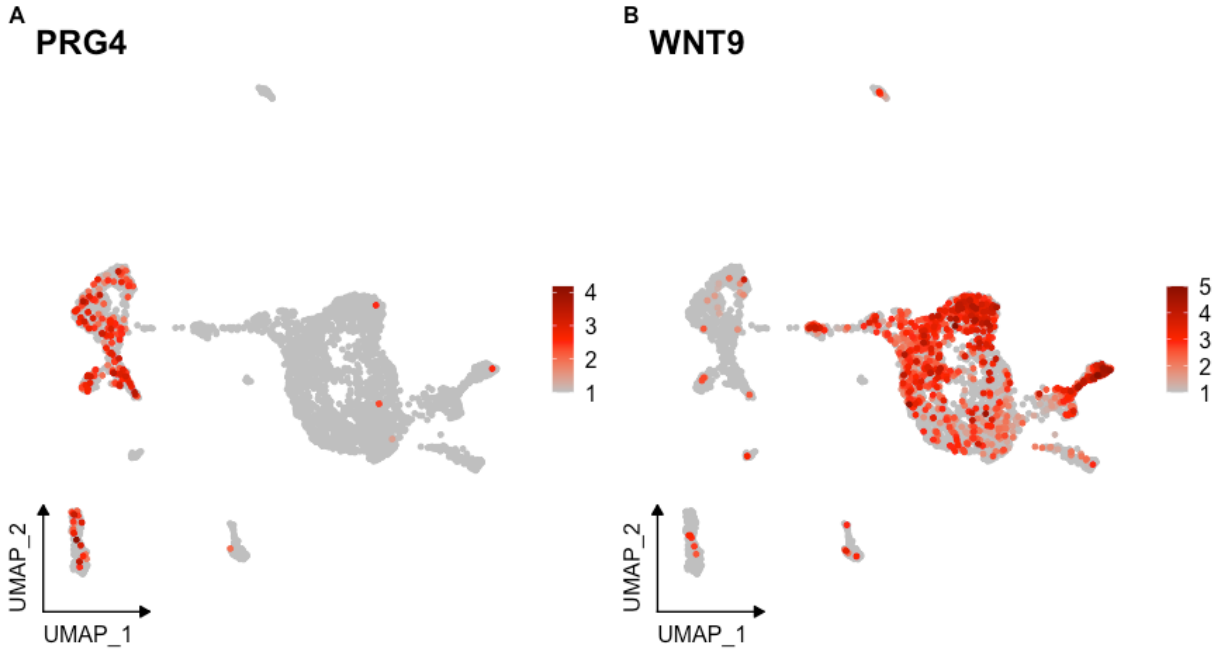

S4 Fig. Expression of marker genes previously documented in the sea cucumber. (A-C) UMAP highlighting the cells expressing (A) Wnt9, (B) SAA, and (C) Proteoglycan-4.

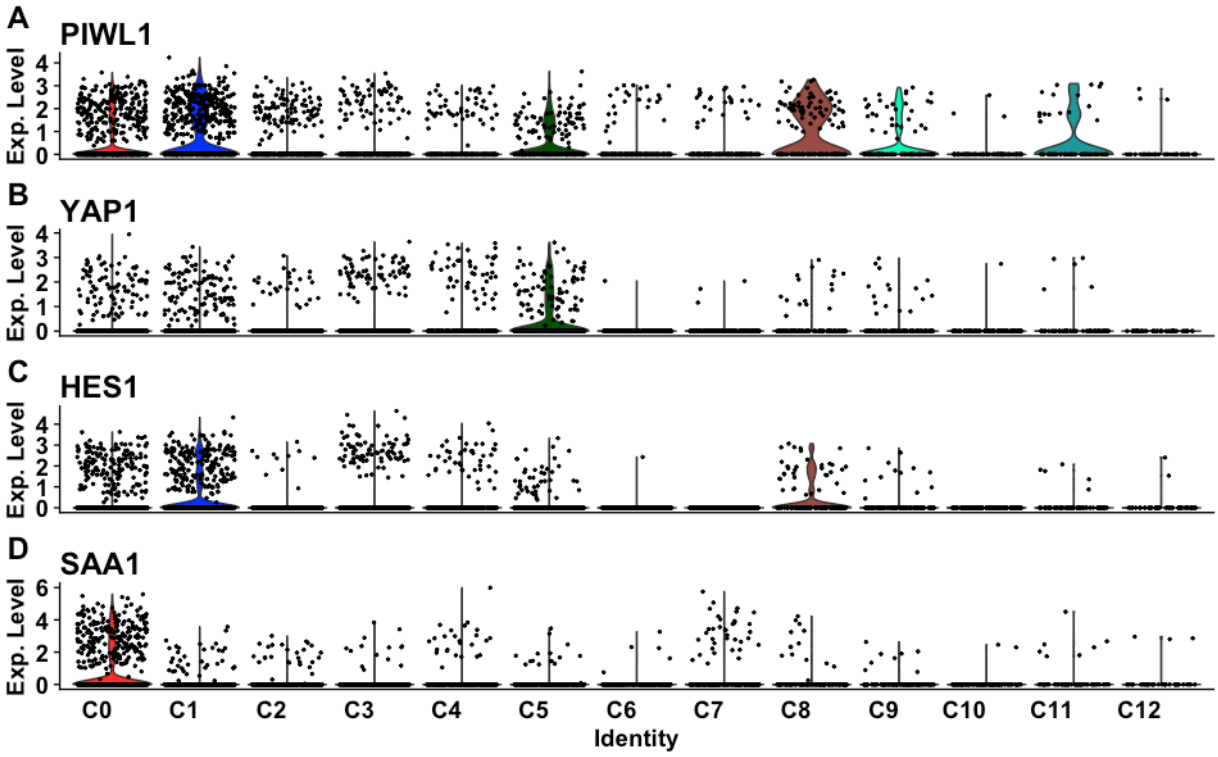

S5 Fig. Expression of marker genes associated with cell types or state. (A-D) Violin plot highlighting the level of expression of (A) PIWL1, (B) YAP1, (C) HES1, and (D) SAA1 across clusters.

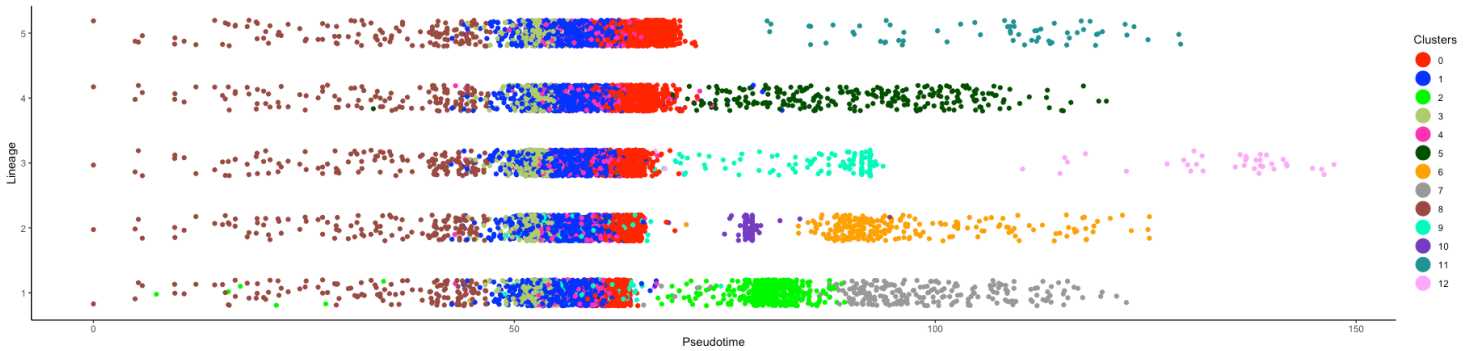

S6 Fig. Pseudotime analysis of all clusters within the 9dpe intestinal regeneration dataset. Each color reflects the corresponding cluster form C0-C12. The x-axis represents slingshot pseudotime and y-axis the corresponding lineage.

1403
1404
1405
1406
1407

S7 Table. Antibody/Markers used for immune- and cytochemical labeling of dissociated cell suspension.			
Antibody/Marker	**Labeling**	**Product No.**	**Reference**
Ab Sph AA12	Coelomocyte	-	Ramírez-Gómez et al., 2010
Ab RN1	Neuronal	-	Nieves-Ríos et al., 2020
Ab GFS	Neuronal	-	Diaz-Balzac et al., 2007
Ab KL14	Mesenchyme	-	In preparation
Ab MESO	Mesothelial cells	-	García-Arrarás et al., 2011
Ab beta tubulin	Neuronal/Cilia	Sigma T5293	Tossas et al., 2014
Ab Acetylated tubulin	Cellular	Sigma T6793	Tossas et al., 2014
Ab alpha tubulin	Cellular	Sigma T5168	Tossas et al., 2014
Fluorescent Phalloidin	Muscle fibers	Sigma P1951	García-Arrarás et al., 2011; Murray and García-Arrarás et al., 2004
Toluidine Blue	Nuclei		

1408
1409
1410
1411
1412
1413